LABORATORY ASSESSMENT OF ASPHALT CONCRETE DURABILITY UTILIZING BALANCE MIX DESIGN

BY

ARTURO FRANCISCO ESPINOZA LUQUE

THESIS

Submitted in partial fulfillment of the requirements
for the degree of Master of Science in Civil Engineering
in the Graduate College of the
University of Illinois at Urbana-Champaign, 2018

Urbana, Illinois

Advisors:

Professor Imad L. Al-Qadi
Dr. Hasan Ozer

ABSTRACT

The national highway network is vital to promote social and economic development in the United States; thus, it is essential to guarantee its durability. Better durability of asphalt concrete (AC) pavements would translate into less maintenance and repair, better ridership quality, and reduced environmental impacts. However, in the current design practice for AC materials, little attention is given to study AC performance and its implications for future durability. Additionally, budget and ecological constraints are continually requiring of pavement engineers to include increasing amounts of alternative materials into AC mixes; their impact on future mix performance, however, might not be captured by current testing approaches. Therefore, improving the tools available to assess AC durability is crucial.

This research studied the laboratory performance of a high-quality Stone Matrix Asphalt (SMA), designed by the Danish Road Directorate, and that of a conventional Illinois dense-graded mix, blended with different dosages of rejuvenator to enhance its performance. The effect of short-term aging on the rejuvenated AC blends was also considered in this research. This study focused on assessing the cracking and rutting potential of the studies mixes using the Illinois Flexibility Index Test (I-FIT) and the Hamburg Wheel Track Test (HWTT). Additionally, mix stiffness and moisture damage susceptibility were evaluated using the output data from I-FIT and HWTT, respectively. The tests results were analyzed using the Illinois Balance Mix Design (I-BMD) approach to evaluate the tradeoffs between flexibility and rutting improvements.

This study found that adding rejuvenator to AC does improve its flexibility characteristics; however, the impact becomes less significant with increasing dosage. However, the flexibility index (FI) exhibited by the SMA was the highest amongst the mixes considered in this study. Aging negatively affects FI, but its impact is somewhat limited. Regarding rutting resistance both types of mixes exhibited similar final rut depths; however, at higher dosages of rejuvenator the dense-graded AC mix becomes excessively soft and experiences rapid failure. Rutting resistance was found to be much more sensitive to the effects of both aging and rejuvenation that FI. Analysis of the moisture susceptibility data revealed that the SMA and the un-modified dense-graded AC mixes were less impacted by moisture damage compared to AC mixes with higher dosages of rejuvenator.

To my parents

ACKNOWLEDGEMENTS

Foremost, I express my gratitude to Dr. Imad Al-Qadi and Dr. Hasan Ozer for their guidance, support, and mentorship during my tenure at the University of Illinois. Being a member of the transportation research group under Dr. Al-Qadi and Dr. Ozer has been one of my most forming experiences, and it has highlighted the importance of good leadership on creating an outstanding work environment.

Also, I would like to acknowledge the support received from friends and colleagues at the Illinois Center for Transportation (ICT) and the University of Illinois: Greg Renshaw, Michael Johnson, Shenghua Wu, Jim Meister, Fazal Safi, Zehui Zhu, Punit Singhvi, Izak Said, Mohammed Sawalha, Kamal Hossain, Edoardo Barber, and to all the UIUC students and staff from ICT who have lend me their friendship and support.

Finally, I would like to thank my family for their support and encouragement along my entire life, in particular, I thank my parents Arturo and Claudia, and my wonderful Charmaine who has truly been my better half by bringing out the best of me.

TABLE OF CONTENTS

CHAPTER 1: INTRODUCTION

1.1 Background

The highway network is a crucial component of the national transportation infrastructure, playing a pivotal role on promoting economic development and growth across the country by allowing access to natural resources, decreasing transportation cost for goods, and facilitating the movement of people to and from production centers *(1)*. However, shrinking budgets, increasing user demand, higher construction and maintenance costs, and a complicated political landscape, have increased the strain on an already aging road network in the USA. The American Society of Civil Engineers (ASCE) 2017 Infrastructure Report Card, rates the USA road network as 'D' which translates into a 'Poor/at Risk' condition *(2)*.

Major factors cited by the ASCE Infrastructure Report Card were overcrowding, underfunding, and poor serviceability; these factors translate into more frequent and prolonged congestions, increasing the man-hours lost by American workers, estimated at 42 hours per driver per year. Higher congestion also leads to higher transportation costs, depreciating the cost of goods. For the USA, it is estimated that by 2030 road congestion could mean a 44% increase in the cost of doing business *(3)*. Finally, congested roads reduce the fuel efficiency of vehicles and increase the concentration of air pollutants in high traffic areas.

Ensuring an adequate level of serviceability for the nation's roads is in the best interest of government agencies and users. However, limited funding is always a lurking challenge that transportation professionals encounter when devising plans for road construction, preservation, and rehabilitation; this highlights the importance of pavement durability. The more a road can last

without the need of significant repair or maintenance, the less funding it will require during its service life, and the more resources can be made available for improving other sections of the network.

Asphalt concrete (AC) is the most used construction material for highway paving projects; it has been the material of choice for road paving due to its low initial construction cost, faster construction expediency, excellent friction and sound qualities, and its easiness for rehabilitation and recycling. AC is a mixture of stone aggregates and liquid asphalt. The aggregate matrix compromises 94-95 percent of the total mixture weight and supplies a skeleton that provides the bulk of the load-bearing capacity. Asphalt coats the aggregate particles to retain them together, and protects them from weathering effects; it contributes 5-6 percent of the total weight of the AC mixture.

For a pavement structure, AC is usually used in the upper layers of the structure, leaving it exposed to higher stress levels and harsher environmental conditions which will eventually induce the development of distresses on the pavement. Pavement distress can be defined as deterioration or distortion of the pavement material which indicates a decline in the surface condition or the overall structural load-carrying capacity of the pavement *(4)*. Surface condition distresses for AC pavement are related to a reduction in road functionality regarding ride quality, noise, and safety; but they do not necessarily affect the load-carrying capacity of the structure. Alternatively, structural distresses are related to a decline in the overall bearing capacity of the structure, negatively impacting the longevity of the road. Two of the most common structural distresses are cracking and permanent deformation.

For AC, cracking occurs when there is a separation of pavement particles, there are different classifications of AC pavement cracks, including fatigue cracking, low temperature cracking, and block cracking; each of them with their own initiation mechanism *(5, 6)*. Binder modification, aggregate gradation changes, increased binder content, usage of AC layers with crack control properties, are some of the topics that have been studied to control the cracking of AC pavement's *(7, 8)*. Permanent deformation is associated with rutting formation along the wheel path, which develops gradually as vehicle repetitions accumulate. Stronger aggregate, stiffer binders, polymer modification, lower binder contents, have been some of the AC variables that can be used to improve rutting performance *(9, 10)*.

1.2 Problem Statement

To improve the durability of AC, different research efforts have been focused on utilizing better quality materials, developing better standards, and improving design methodologies. However, there still a knowledge gap between balancing the effects of mix design modifications with the inclusion of non-standard materials such as additives and recycled materials, and their impact on rutting and cracking resistance. In general, improving one of these characteristics will negatively affect the performance of the other. With a better understanding of how different mix design variables, such as gradation type, binder grade, amount of recycled materials, and aging, affects AC pavement rutting and cracking potential, practitioners will be able to balance the performance of AC mixtures better, resulting in more durable and long-lasting pavements.

1.3 Research Objective and Scope

This study intends to expand the understanding of how performance-based tests can be used to study mix durability regarding rutting and cracking potential. In particular, this research focuses on the following objectives:

- Investigate the effects of short-term aging on mix performance, and evaluate the effectiveness of using recycling agents as a strategy to improve the durability of AC.
- Evaluate the performance of high-quality AC materials such as Stone Matrix Asphalt (SMA) as compared to conventional AC mixes.
- Assess the influence of mix design variables, aggregate size, binder type and content, and air voids, on expected AC performance.
- Study the applicability of a balance mix design approach as a tool to evaluate AC performance.

In this study, mix durability was studied considering cracking and rutting laboratory performance. Cracking means the formation of a discontinuity in the material, for this research cracking susceptibility was evaluated using the Illinois Flexibility Index Test (I-FIT). Additionally, from the I-FIT output, a secant modulus was obtained and used as an indicator of AC stiffness before crack propagation. Rutting refers to the formation of a depression along the wheel path on the surface of the pavement, the Hamburg Wheel Track Test (HWTT) was used to assess the rutting potential of the various AC materials studied. Also, using the HWTT output, a moisture susceptibility analysis was included in this study due to its potential influence on both cracking and rutting potential, and its overall impact on mix durability.

Traditionally, mix design methods are primarily based on achieving a predetermined set of volumetric parameters. In this study, a balanced mix design was used. Balance mix design is a methodology that evaluates AC performance on multiple modes of distresses simultaneously. The I-FIT and HWTT results were compared using the Illinois Balance Mix Design (I-BMD) approach to study the applicability of this method as a tool to evaluate AC durability.

CHAPTER 2: CURRENT STATE OF KNOWLEDGE

2.1 Asphalt Concrete Mix Design

For centuries, asphalt has been used as a construction material due to its adhesive and waterproofing characteristics; however, its application for roadway construction, where is used as a blend of asphalt and mineral aggregates, has started more than a century ago and followed the introduction of the automobile. An asphalt concrete (AC) mixture, also referred to as Hot-Mix Asphalt (HMA), consists of liquid asphalt (binder), fine and coarse aggregates (sand and gravel), and optional additives that can be used to improve its engineering properties. The purpose of mix design is to select the optimum amount of asphalt content for a desire aggregate blend, meeting a predefined criterion. This section reviews the historical design methods that have been used in the United States, together with the current design practice, and the various methods to evaluate AC performance.

2.1.1 Hveem Method

In the late 1920's, mix design in California relied on the determination of the appropriate amount of asphalt based on the judgment of an experienced engineer who would know how a mix with the correct amount of asphalt should look. To overcome the subjectivity of the engineer's judgment method, in 1927 F. N. Hveem was assigned by the California Division of Highways to develop a procedure that could determine the adequate amount of asphalt for any aggregate gradation. The final blend should deliver a "hard and smooth" road surface that will not deform under traffic *(11)*.

The Hveem method consists of obtaining an initial estimate for the optimum 'Asphalt Binder Ratio' *(12)* and testing the stability and cohesion properties of the proposed mix. These results are used to evaluate the compliance of the mix against predetermine specification *(13)*. The stability test consists of subjecting a cylindrical specimen to vertical loading and measuring the horizontal deformation based on the lateral pressure that the specimen induces to an enveloping fluid. The deformation experienced by the specimen is correlated with the vertical and horizontal pressures to obtain a 'Stabilometer Value'. The cohesion test relies on applying a constantly increasing bending moment, to a specimen until breakage. The amount of mass used to generate the moment required to break the specimen is recorded and correlated with the specimen dimensions to obtain a 'Cohesion Value'.

The Hveem design method was an early effort to correlate future AC field performance to laboratory testing results. One of the main advantages of the Hveem design method was that it could discriminate between different mixes based on their simulated performance with the stabilometer test. However, the stability test was more related to internal friction properties of the aggregate structure, and asphalt content, than to the binder grade properties *(14)*. Additionally, the testing equipment was considered somewhat expensive and not portable. Finally, essential mixture volumetric properties related to mixture performance, such as air voids, were not routinely determined. The combination of these factors was believed to have caused 'dry' mix designs, with low asphalt contents, resulting in poor AC durability *(15)*.

2.1.2 Marshall Method

Bruce G. Marshall originally developed the Marshall Method during the 1940's working with the Mississippi State Highway Department, and the U.S. Army Corps of Engineers later refined it. The principal motivation for the development of this method was to establish a mix design procedure that uses simple and readily available test equipment to evaluate volumetric and strength related properties of AC mixes *(16)*. The practicality of the Marshall method made it the most widely used mix design procedure in the United States for many decades, and it still used in many countries around the world.

Marshall method relies on preparing multiple mix samples at different asphalt contents and evaluating the mix design regarding following properties: stability, flow, density, voids in the mineral aggregate (VMA), voids filled with asphalt (VFA), and total air voids (AV). The final design is selected at the optimum asphalt content that satisfies all the criteria for the different mix properties *(17)*.

One of the main advantages of the Marshall method is that it tries to balance volumetric requirements (AV, VMA, VFA, density) with performance-related testing (stability and flow). Stability and flow are measured by subjecting a small unconfined cylindrical specimen to uniaxial loading until breakage. Stability is taken as the maximum load sustained by the sample, and it has been correlated to the strength of the material. Flow is recorded as the amount of deformation undergone by the specimen before failure, and it is an indication if the mix is overly asphalted or not *(18)*.

Despite its success and broad adaptation, the Marshall method is not without its shortcomings. Specimen preparation relies on compacting samples using a blow hammer that compacts the material with impact action, which is not representative of actual field compaction *(15)*. Additionally, it has been shown that the specimens' surface texture alters the uniformity of the load applied from the Marshall strength test *(14)*. Also, the test has had poor correlation to the actual permanent deformation resistance of the mixes, and may not be able to classify the mixes accordingly *(19)*. The aforementioned shortcomings of the Marshall method are believed to have resulted in the design of binder-rich AC mixes which lead to the so-called 'Rutting Epidemic' on US roads during the 1980's *(15, 20–22)*. The Strategic Highway Research Program (SHRP) spearheaded the development of a new mixture design method, Superpave, to alleviate the rutting problem present across the nation.

2.1.3 Superpave System

Superpave is a result of a 150 million dollars research effort under SHRP with the final goal of improving the performance of highway infrastructure. One of the areas is optimizing AC mixture resistance to permanent deformation, fatigue cracking, and low temperature cracking. The system consists of three interrelated areas: (1) performance-graded asphalt binder specification and tests; (2) aggregate quality criteria; and (3) a mixture design based on volumetric properties, using a gyratory compactor, together with performance evaluation *(20)*.

The development of Performance Grade (PG) binder grading, was one of the most significant outcomes from the Superpave development. Before the PG system, binder grading relied on empirical methods such as penetration testing, or viscosity classification which did not capture

useful engineering qualities of the binder; additionally, there was little or no consideration for temperature and aging effects on binder behavior *(23)*. The battery of test used on the PG system measures the performance of the binder at different aging stages, original, short-term, and long-term; and it also assesses different engineering properties, construction workability, rutting potential, fatigue and thermal cracking potential. The main advantage of the PG system is facilitating asphalt binder testing at extreme temperatures related to those expected during service and evaluate performance at various stages of its life *(24)*. Figure 2.1 summarizes the type of tests and aging conditions at which they are conducted; where: RV – Rotational Viscosity, DSR – Dynamic Shear Rheometer, DTT – Direct Tension Test, BBR – Bending Beam Rheometer, RTFO – Rotational Thin Film Oven, PAV – Pressurized Aging Vessel.

In the case of mineral aggregates, Superpave has so-called 'consensus' properties which are determined by expected traffic conditions; such properties include angularity, flat and elongated particles, and clay content. Also, characteristics related to the source of the aggregate source are also evaluated, such as toughness, soundness, and deleterious materials. Regarding aggregate gradation, Superpave uses a 0.45 power gradation chart and provides control points and a restricted zone to avoid the use of undesirable gradations, which can result in tender mixes *(25)*.

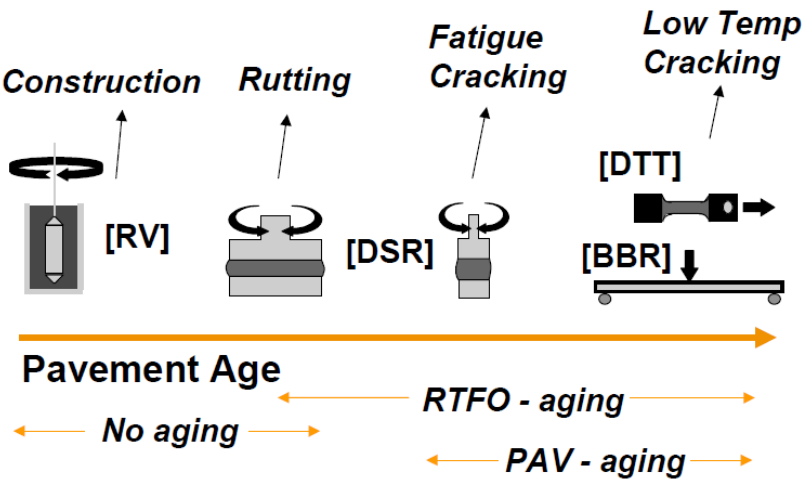

Figure 2.1 Asphalt PG system tests *(15)*

The third major component of Superpave is about AC design. The overall objective of the method is to develop a well-performing, workable, and durable mixes; this is achieved by attaining required volumetric properties, using the adequate amount of compaction corresponding to expected traffic level, and evaluating mix performance *(26)*. For volumetrics, the fundamental variables are design air voids (AV_{des}), voids in the mineral aggregate (VMA), voids filled with asphalt (VFA), and the Dust-to-Binder ratio *(27)*. AV_{des} refers to entrapped air within the AC mix and is a measure of mix density; it is commonly used as 4% for design purposes. VMA is the space within the aggregate structure that is available to accommodate the binder, minimum values for VMA are given depending on the gradation size. VFA is the percentage of the volume of the VMA that is occupied by the effective binder (VBE), and its value range is dependent of the expected traffic level at which the mix would be subjected. Dust-to-Binder ratio influences the total amount of aggregate surface area and the amount of permeability of the AC mix. The ratio is the relationship between the weight of the aggregate finer than 75μm to the weight of the effective binder in the mix. Satisfying the requirements for these volumetric properties should be achieved at the adequate compaction effort,

measured by the design number of gyrations of the Superpave Gyratory Compactor (SGC); the design gyrations is related to the expected service-life traffic level *(28)*.

Achieving the required volumetrics at the design gyration level is influenced by the aggregate gradation, mineral source, and binder content in the mix; all these variables have been correlated to mix performance *(29)*. Finally, once the AC volumetric requirements are satisfied, Superpave includes the evaluation of potential mix performance using a moisture susceptibility test *(30)*.

The original conceptualization of Superpave included further evaluation levels dependent on traffic intensity, from Level 1 to Level 3 *(31)*. Level 1 was based on volumetric mix design. Level 2 included performance tests which measure engineering properties. Level 3 added a full set of materials characterization testing. In current Superpave practice, only level 1 design is fully implemented; while from levels 2 and 3 only moisture susceptibility, and to some extent permanent deformation evaluation, are included in current practice.

The adoption of Superpave mix design method did aid in reducing the amount of rutting presence in the US, which was related to AC mixes designed with the Marshall method; however, the national road network now faces a widespread problem of pavement cracking *(29)*. To overcome the problems regarding pavement cracking, while maintaining adequate rutting characteristics, recent research efforts have been moving towards design methodologies that incorporate performance prediction, such as balance mix design that considers both rutting and cracking of the AC mixes.

2.1.4 Balance Mix Design

The introduction of Superpave method led to AC mix designs with lower asphalt content and coarser aggregate matrices, reducing rutting occurrence. However, these type of mixes brought their own set of challenges, namely, early-age cracking, poor workability and compatibility, and overall reduce durability. These three problems are interrelated since a poorly workable mix is difficult to compact, resulting in higher air voids, which bring higher permeability and age hardening, reducing cracking resistance *(32)*. A practical solution could be to merely add more binder since it has been shown that AC mixes rich in asphalt binder significantly improve their workability, durability, and cracking resistance. However, adding more binder induces higher costs and negatively impacts permanent deformation resistance *(33)*. Additionally, new designs are not only using the traditional components, but there is an increasing usage of recycled materials, additives, and fibers. The impact of alternative components on AC performance might not be adequately evaluated by volumetric analysis only.

To address these new challenges, there is a renewed research interest in establishing design criteria that not only assesses mix volumetrics but also evaluates laboratory mix performance. Balance mix design (BMD) is defined as "AC mix design using performance tests on appropriately conditioned specimens that address multiple modes of distress taking into consideration mix aging, traffic, climate and location within the pavement structure" *(34)*. It is a topic of current research focus as highlighted by the National Cooperative Highway Research Program project 20-07 *(35)*, and multiple efforts from state agencies *(36, 37)*.

The principle of BMD relies on evaluating the laboratory performance of the proposed mix design, using laboratory tests that have been related to future field performance against known distress types such as rutting and cracking. For Rutting, HWTT is the most common performance test already adopted by many state agencies. For cracking, however, multiple tests can be used, the selection of any of them depends on the specific crack initiation mechanism and environment of interest *(38)*.

There are three main approaches for the implementation of BMD, (1) volumetric design with performance verification, (2) performance-modified volumetric design, and (3) performance design *(34)*. Performance verification follows Superpave design, based on AASHTO M323 *(27)*, but incorporates performance testing criteria that the proposed mix must pass or it should be redesigned. Performance-modified refers to designing a mix following M323, and if the performance tests results are not satisfactory, adjustments to the volumetric proportion should be made. Performance design relies entirely on performance test results to select the adequate binder content for the mix. Figure 2.2 shows a workflow summarizing the steps for the three approaches.

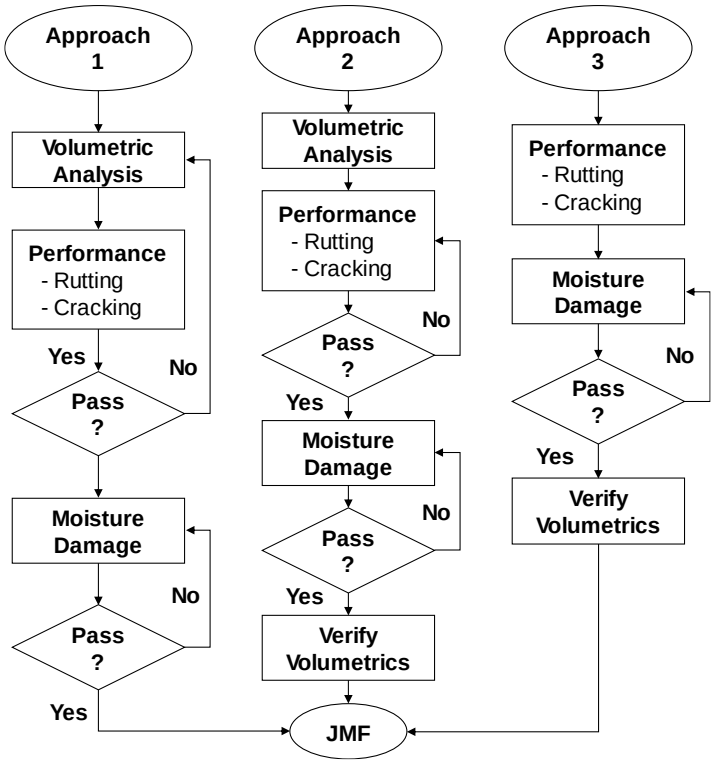

Figure 2.2 Mix design workflow for the different BMD approaches (JMF = Job Mix Formula)

BMD promises to bridge the gap between the known effects of volumetric variables on AC durability with laboratory testing that relate mix performance to distress resistance in the field. The central challenge for BMD implementation is to broaden the correlation of laboratory testing results to actual field performance and to define an adequate cracking test, or set of tests, that tackles the needs of each agency and contractor involved.

2.2 Asphalt Concrete Durability

AC durability can be defined as the ability of compacted AC to maintain its structural integrity when exposed to environmental effects and traffic loading. AC durability is affected by mechanical responses of materials, interactions between structure and materials, and the influence of non-load

related mechanisms such as oxidative aging and moisture damaged *(39)*. This section presents some of the principal distress types and mixture properties that affect AC durability.

2.2.1 Pavement Cracking

Cracking occurs when there is a separation of pavement particles; it is a primary mode of distress on pavements, and widespread cracking presence is usually a trigger for pavement maintenance or rehabilitation *(40)*. The four fundamental modes of cracking initiation on AC pavements are thermal, reflection, and fatigue, including near surface.

Thermal cracking, which is usually transverse to the direction of traffic, is caused by tensile stress formation in the AC due to low temperatures cooling cycles. The contractions induced by cooling result in thermal tensile stress development in the restrained surface layer, and it is highest in the longitudinal direction of the pavement *(41)*; hardening/aging of the AC mix exacerbates the cracking potential of the layer.

Reflective cracking is one of the main distresses for asphalt overlays. Existing joints or cracks on underlying layers can induce reflection cracking primarily by stress concentration phenomena, and secondarily, by allowing excessive deflection at the crack *(42)*.

Fatigue cracking initiates at the bottom, middle, or top of AC layer and propagates with repeating cycles; it first reflects on the surface as short longitudinal cracks in the wheel path that then quickly spread and become interconnected, forming a net type cracking pattern on the surface. This type of cracking is generated by the continuous bending of the AC layer which generates tensile stresses at

the bottom of the layer until a crack is initiated; with repetitive loading, the crack grows until it reaches the surface *(43)*.Some of the mechanisms causing crack formation are shearing of the AC near the surface where the tire contact stresses are relatively high. Severe aging of the AC surface resulting in extreme stiffness that, in combination with high contact stresses, induce cracks adjacent to the tire edge *(44)*.

Traditional design methods that relied on volumetrics analysis provided some level of certainty against crack-related durability issues, mainly by controlling density and the amount of effective binder; however, new AC mix designs have become more intricate due to the incorporation of recycled materials, recycling agents, binder additives, and warm-mix asphalt technologies. The effect of these material types on AC goes beyond adjusting volumetrics, which highlights the importance of incorporating a balance mix design approach.

2.2.2 Pavement Rutting

Pavement rutting is associated with the formation of a channel type depression along the wheel path. This type of distress reduces the pavement serviceability and creates hazardous driving condition since the accumulation of water on the wheel-path ruts can create hydroplaning conditions *(43)*. Rutting can be the result of AC densification, plastic shear deformation, or a combination of both *(45)*.

Rutting is developed across multiple stages. The first stage is post-compaction consolidation which appears in the early-life of the payment, and it is driven by the reduction of air voids within the matrix of the material. The effect of post-compaction consolidation subsides when the density of

the AC reaches a point where the material structure becomes stable. Plastic deformation drives the second and third stages and occurs after the post-compaction consolidation effect has settled. The second stage is characterized by a constant increase of rut depth with increasing number of load repetitions; this section is commonly referred as the 'Stable Zone' or 'Creep Phase'. The third and final stage, presents rapid rut progression as the structural integrity of the material is compromised; this stage is known 'Failure Zone.' The moisture presence accelerates the appearance of the third stage by inducing particle stripping.

Major factors affecting permanent deformation are the pavement structure (layer thicknesses and quality), traffic load and volume, initial field compaction, and environmental effects such as moisture and temperature *(46)*. There has been extensive research to improve the permanent deformation resistance of AC. Using stronger aggregate, stiffer binder types, polymerized asphalt, or lower binder contents, are some of the strategies that have been proven to improve the rutting resistance of AC *(47–49)*. However, one of the preeminent variables that have contributed to reducing AC permanent deformation has been the addition of recycled materials such as reclaimed asphalt pavement (RAP), and recycled asphalt shingles (RAS). These materials possess severely-aged asphalt which is much stiffer than the binder grades with which AC is usually prepared. Adding even moderate amounts of aged asphalt to AC increases the overall binder stiffness of the mix which in turns reduces permanent deformation susceptibility *(32, 50, 51)*.

2.2.3 Moisture Susceptibility

Moisture damage is defined as the loss of strength and stability caused by the active presence of moisture, and it severely affects the durability of pavements. Using additives or modifiers is the

most common technic used to mitigate the potential for moisture damage *(52)*. Moisture damage is not considered as a failure mode by itself, but rather is a condition that accelerates the appearance of other types of distresses. Moisture presence in AC induces the separation of the asphalt film from the aggregate particles causing stripping. The widespread presence of stripping reduces the cohesive and adhesive characteristics of the AC pavement layer, diminishing its structural capacity and distress resistance *(53)*.

In the current Superpave mix design methodology, moisture susceptibility evaluation is one of the few performance tests that are required for every design. Moisture damage is evaluated via the tensile strength ratio (TSR), which is the relationship between the indirect tensile strength of conditioned (water saturation, and freeze-thaw cycle) and un-conditioned specimens *(30)*. Another way to assess the moisture susceptibility of AC is to evaluate the stripping inflection point (SIP). The SIP, which believed by some as related to stripping, is obtained at the intersection of creep slope and the stripping lines obtained from the rut progression curve of the HWTT results *(54)*.

2.3 Asphalt Concrete Aging

Asphalt binder is an organic compound which naturally oxidizes with time; this oxidation is what is known as aging *(55)*. It has been documented that when asphalt binder is aged, there is a change in its chemical group's composition; there is an increase in the asphaltene fraction while the aromatic portion decreases *(56)*. Asphalt binder undergoes a rapid increase (“initial spurt”) in viscosity during the first stages of aging, and then the rate settles at a constant rate (steady state) *(57)*. This effect has been attributed to the fact that asphalt binder’s more volatile parts react first, and the less reactive groups experience oxidation reaction later *(58)*. This change in chemical

groups can be measured using Infrared (IR) spectroscopy, where an increase in the carbonyl chemical functional group may be observed *(59)*. As the carbonyl group presence increases, it suggests a higher concentration of asphaltenes in the binder *(60)*.

The increase of asphalt binder hardiness with age, or age hardening, turn the material stiffer and more brittle, making it prone to cracking, reducing the overall durability of the pavement. In the field, it has been well documented that age hardening is increased when there is high permeability of the pavement *(29)*. When there is high in-place permeability, there is an increased presence of air and water which will generate higher rates of oxidation with the asphalt coating, accelerating the pace of age hardening. Another aspect that affects the age hardening process is the binder film thickness that coats the individual aggregate particles; in general, AC mixes with thinner binder films have been shown to be more susceptible to oxidation, and consequently display poor durability, as compared to mixes with ticker binder films *(32)*.

In addition to the natural age hardening that AC undergoes while in service, the increasing amount of recycled asphalt materials such as RAP and RAS adds a considerable amount of age-hardened asphalt to new AC mixes. Although the primary motivations to add recycled materials are economical, since asphalt binder is the most costly component of AC, or environmental, by reducing the amount of virgin material requirements, multiple studies have acknowledged that the incorporation of these age-hardened materials increase the stiffness and brittleness of AC *(9, 51, 61–63)*. Rejuvenators have been introduced to counterbalance the detrimental effects of aging on AC.

2.3.1 Rejuvenators for Asphalt Concrete

To restore some of the mechanical properties of asphalt binder that have been lost due to aging, it is common to blend recycled asphalt with recycling agents known as rejuvenators. If the appropriate amount of rejuvenator is added and adequately mixed, the recycled asphalt binder may meet the target performance grade (PG), resulting in improved cracking resistance of the AC mixture without adversely affecting its resistance to rutting *(64)*. In general, rejuvenators are assumed to act by replenishing the volatiles and light bitumen fractions that have been lost during the life of the recycled pavement. The recovery of the mechanical properties of binder-rejuvenator blends is commonly attributed to the restoration of the asphaltene-maltene ratio *(65)*. Some of the most common sources for rejuvenators are either low viscosity waste materials or 'Engineered' products *(66)*. Table 2.1 summarizes the types of rejuvenators by chemical source.

The interaction dynamics between rejuvenators and asphalt binder have mostly been studied at a binder level by assessing the mechanical and chemical properties of the binder-rejuvenator blends *(67–70)*; this method permits the understanding of how much different recycling agents can improve the condition of aged asphalt binder. However, in practice, rejuvenators are used directly into AC mixes, by combining it with RAP material at the mixing plant *(50)*, as a surface treatment *(71)*, or as an additive while performing in-place recycling *(72)*.

Table 2.1 Types of AC rejuvenators *(73)*

Category	Examples	Description
Paraffinic Oils	Waste Engine Oil (WEO) Waste Engine Oil Bottoms (WEOB) Valero VP 165® Storbit ®	Refined used lubricant oils
Aromatic Oils	Hydrolene ® Reclamite ® Cyclogen L ® ValAro 130A ®	Refined crude oil products with polar aromatic oil components
Naphthenic Oils	SonneWarmix RJ ™ Ergon HyPrene ®	Engineered hydrocarbons for asphalt modification
Triglycerides & Fatty Acids	Waste Vegetable Oil Waste Vegetable Grease Brown Grease Oleic Acid	Derived from vegetable oils
Tall Oils	Sylvaroad™ RP1000 Hydrogreen ®	Paper industry byproducts

Understanding the blending quality and rejuvenator diffusion is a research area that has attracted research attention *(66, 74)*. Since the amount of rejuvenators used on AC is low compared to the main components of a mix, usually 5% to 10% of binder weight which would represent a 0.25% to 0.60% component by total weight of the mix, a meaningful effect on the total volumetric properties of the mix is not expected. However, mix performance can be significantly altered. Applying performance-based analysis approaches such as BMD could improve the effectiveness of how rejuvenators are used.

2.4 Stone Matrix Asphalt

Stone Matrix Asphalt (SMA) is a tough, stable, rut-resistant, gap-graded mixture that relies on stone-to-stone contact to provide strength, and a binder and filler-rich mortar to provide durability *(75)*. SMA provides better performance in wet weather as it produces lower splash and spray

between the tire and wet pavement; also, SMA shows reduced noise levels, compared to traditional dense-graded mixes *(76)*.

Some of the distinctive features of SMA are a gap-gradation, that maximizes stone-on-stone contact (reducing rutting potential); high-quality aggregates that minimize particle breakage; and a rich mastic blend created by high filler and binder content *(77)*. Due to its premium qualities, SMA has been used to improve the overall durability of AC pavements, and its superior performance, in terms of low rutting potential and high cracking resistance, has been documented by multiple studies *(77–80)*.

SMA can be produced and compacted using the same type of equipment used for conventional AC. However, better quality aggregate, higher binder and filler contents, and the used of fiber to avoid drainage, increase the production cost of SMA *(81, 82)*.

CHAPTER 3: RESEARCH METHODOLOGY

3.1 Experimental Set-Up

The necessity to estimate future AC mix performance, and the incorporation of increasing amounts and types of non-standard materials, such as recycled materials, additives, or modifiers; are industry trends that have motivated the re-evaluation and updating of AC mix design methods. Balance mix design holds the promise of facilitating the understanding of mixture performance. However, the test results used for a balance mix design analysis must be interpreted within a set of boundaries related to extensive materials testing results, highlighting the relevance of expanding the testing matrix available by including different types of mix designs and testing conditions.

The experiment carried in this study has the objective of evaluating the practicality of using the Illinois Balance Mix Design (I-BMD) approach as a discrimination tool to decide what type(s) of AC mixes possess the highest durability potential by studying the cracking and rutting potential of various mix types, and the effect of various aging conditions, density levels, and rejuvenator dosages. Two types of AC mixes were evaluated in this study, a traditional dense-graded mix, and an SMA. Based on the previous research described in Chapter 2, it is expected that the SMA would have superior performance compared to a dense-graded mix. However, there are not many studies which directly compare SMA versus dense-graded mixes using a balance design approach.

Since the amounts of rejuvenator used in AC are usually low compared to the main mixture ingredients, a significant effect on volumetric properties is not expected; thus, a mix blended with rejuvenator might still satisfy traditional Superpave criteria, but the impact on mix durability is less evident. A key advantage of I-BMD is that it can assess the impact that non-standard materials,

which do not tend to influence mix volumetrics significantly, have on mix performance. To that end, this study also evaluated the effect of using different rejuvenator dosages on AC performance. The rejuvenated mix samples performance was compared to the results of the unmodified sample. Also, a comparison between Un-Aged (UA) and Short-Term-Aged (STA) samples was performed to evaluate the performance progression of AC mixes having rejuvenators with aging.

The concept of BMD is based on evaluating AC performance using laboratory tests that assess mix characteristics that tend to go in opposite directions when some of the mix design variables are altered, or when recycled materials or additives are added. Therefore, the most commonly used approach for BMD implementation is to evaluate mix performance regarding cracking and rutting potential simultaneously. For the I-BMD analysis in this study, the Illinois Flexibility Index Test (I-FIT) was used for cracking susceptibility evaluation, and the Hamburg Wheel Track Test (HWTT) was used for assessing potential rutting. Additionally, a stiffness measure, based on the concept of secant modulus, which can be obtained from the I-FIT output, and a moisture susceptibility indicator, using SIP values obtained from HWTT, were included in the analysis to expand the performance characterization of the AC mixes.

3.2 Testing Materials

The materials used in this study comprehend two types of AC mix designs, a traditional dense-grade type, and an SMA. The SMA had three alternative mixture designs, and the dense-grade mix had a single mix design. The rejuvenator used in this study is a commercially available product. Only one AC mix type and one rejuvenator were used in this study to evaluate the effectiveness of the I-BMD approach in evaluating AC mixtures' performance.

3.2.1 Stone Matrix Asphalt Designs

Three SMA's were analyzed in this study. These mixes were obtained from the Danish Road Directorate (DRD), who used them in their research project "CO_2 emission reduction by exploitation of Rolling Resistance (RR) modeling of pavements" (COOEE). The COOEE project was initiated in 2011 in Denmark with the goal to establish the technical background to develop pavement types that minimize RR. The objective of minimizing RR from the tire-pavement interaction is to reduce the power demand to vehicles, which will require less fuel burning, reducing CO_2 emissions coming from the transportation sector *(83)*. The COOEE project mixes were developed to produce a durable surface course and to minimize their RR properties. Their aggregate size and the type and amount of filler have been optimized to reduce the movement of stone particles while maintaining adequate mix texture and workability *(84)*. Assessing mix durability, was not the central objective of the DRD project.

The mixes studied in this project were designed by the Scandinavian contractor NCC Roads A/S using the Marshall method; they are identified as SMA8 Ref, SMA8 COOEE, and SMA6 COOEE. Table 3.1 presents the main mix design parameters, Table 3.2 illustrates the particle size distribution, and Figure 3.1 shows the design gradation for each of the AC mixes. The original mix designs are attached in Appendix A.

Table 3.1 Mix-design variables of COOEE project

Variable/Mix Type	SMA8 Ref	SMA8 COOEE	SMA6 COOEE
NMAS[1] (mm)	8	8	6
Binder Type[2]	PEN 70/100	PMB 40/100-75	PMB 40/100-75
Binder Content[3] (%)	7.0	7.4	7.9
Air Voids[4] (%)	2.7	2.5	2.4

[1] NMAS: Nominal maximum aggregate size
[2] PEN: Penetration grade (un-modified); PMB: polymer-modified binder, PEN grade
[3] Binder content as per design
[4] Air voids as per design

Table 3.2 Particle-size distributions for COOEE mixes

Sieve Size (mm)	SMA8 Ref	SMA8 COOEE	SMA 6 COOEE
11.2	100	100	-
8	93	95	100
5.6	54	60	96
4	38	46	64
2	25	32	24
1	18	23	18
0.5	14	18	15
0.25	11	14	13
0.125	9	12	12
0.063	8	10	10

The testing performed on the SMA's was carried on Plant-mix lab-compacted (PMLC) specimens. Test specimens for mixes SMA8 Ref and SMA8 COOEE were prepared at two air-voids levels (AV): 4.5% ± 0.5%, and 6.0% ± 0.5%; specimens for SMA6 COOEE were only prepared at 6.0% ± 0.5%. Air void levels were decided based on after-construction density levels from the field test sections in Denmark. After construction, field cores were extracted to evaluate the densification after paving. For mixes SMA8 Ref and SMA8 COOEE, the average AV obtained was 4.5%, while for SMA6 COOEE the average was 6.0%. Therefore, mixes SMA8 Ref and SMA8 COOEE were tested at 4.5% air voids in line with their after-paving densification, and at 6.0%, for comparison

with SMA6 COOEE, which was only evaluated at 6.0%. It is important to mention that, in general, SMA performance tests are commonly done on specimens at 6.0% AV *(75)*.

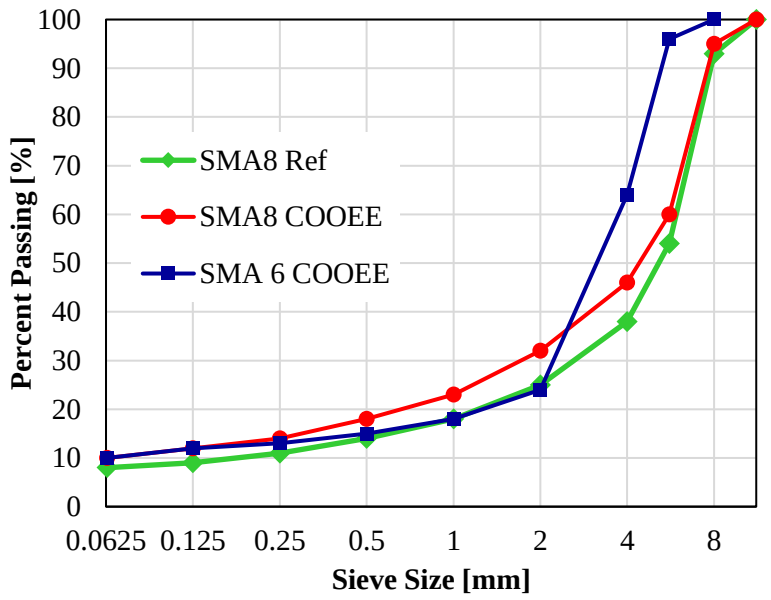

Figure 3.1 Design gradations for COOEE mixes

The binder types used for the design of the DRD mixes were classified using the traditional PEN grade system. Since binder grade has a significant influence on mix performance, it was essential to obtain the PG grade of the binders so that the interpretation of the mix tests results could be more consistent.

The background for the PG system was introduced in Chapter 2, and it follows the standard specification ASTM D6373 *(85)*. For this study, only dynamic shear rheometer (DSR) and bending beam rheometer (BBR) tests were performed. The Multiple Stress-Creep Recovery (MSCR) test was also performed, following ASTM D7405 *(86)*. The primary outcomes of the test are the nonrecoverable compliance (J_{nr}), the percent recovery (%R), and the nonrecoverable compliance difference ($J_{nr,\,diff}$). J_{nr} has been shown to be a better indicator of permanent-deformation resistance,

%R is used as an indication of the degree and type of polymer modification of the binder, and $J_{nr,diff}$ may be used to assess the stress sensitivity of the binder *(87)*. All binder tests were performed on fresh binder samples. Figure 3.2 summarizes the battery of tests performed on the SMA materials.

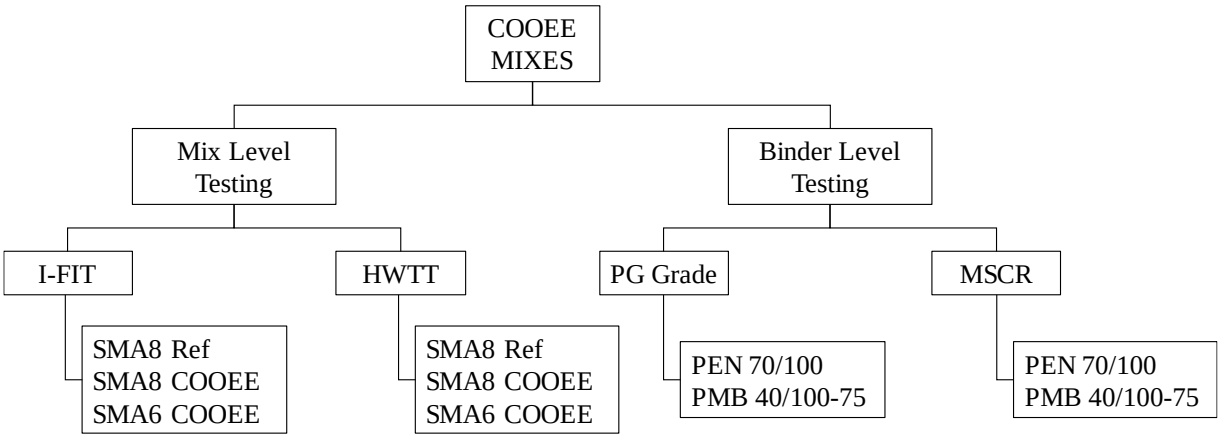

Figure 3.2 Set of tests for COOEE mixes

3.2.2 Dense-Graded Mix

The dense-graded AC mix used in this study was designed per the Superpave method, using 50 gyrations and an NMAS of 9.5 mm; hence, the mix is identified as "N50". The binder type and content are PG 64-22 and 5.9%, respectively. This mix, which is commonly used in the region, was supplied by a local contractor in Champaign County, IL. It has a moderate amount of RAP, 15%, and no RAS. The mix was also selected to study the effect of rejuvenation and aging on mix durability. Testing was also performed on PMLC specimens. The mix was stored in sample bags containing 20 to 25 kgs each. The air void target range for the specimens was 7.0% ± 0.5%, which is a common practice for laboratory testing of initial pavement performance. A copy of the original mix design is presented in Appendix A.

For this study, three mix-rejuvenator blends were prepared by adding 3%, 6%, and 9% of rejuvenator by weight of the total binder content, recycled and virgin binder, as reported in the mix design. The rejuvenator was directly poured into hot loose mix batch and stirred using a mechanical mixer. The blending of the rejuvenator was carried after the loose mix samples were split and had completed 1.5-hr of conditioning in a forced-draft oven at a temperature of 135°C ± 3°C. After blending, the samples were reintroduced into a forced-draft oven for an additional 30 minutes to complete a 2-hr conditioning cycle, which was intended to allow the mix to achieve the compaction temperature range. The described blending methods were devised to achieve a better mixing and dispersion of rejuvenator in the mix. The test results of the different blends were compared to a control blend, which contained no rejuvenator.

To evaluate the effect of STA, after various rejuvenator dosages were blended, additional material samples were kept for an additional 2 hours on a forced-draft oven at a temperature of 135°C ± 3°C, which is the temperature specified in AASHTO R30 for AC short-term conditioning *(88)*. Figure 3.3 presents a flowchart summarizing the specimen preparation and conditioning methods.

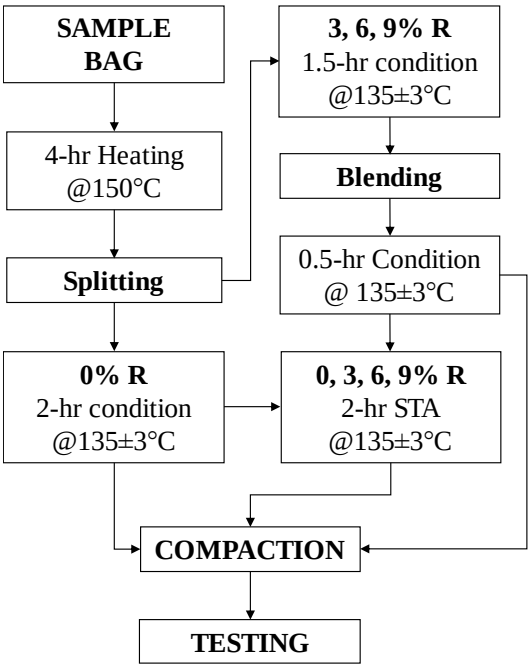

Figure 3.3 Specimen preparation steps, R = Rejuvenator

3.2.3 Rejuvenator Characteristics

The rejuvenator used in this study was a paraffinic distillate solvent extract with the appearance and viscosity of a dark brown lubricating oil. Chemically, it is composed of different hydrocarbons; with aromatic hydrocarbons being the primary component (>75%). It is also virtually free of asphaltenes, which are the particles that have been more closely related to increasing binder stiffness. A high aromatic fraction and a low concentration of asphaltenes are characteristics that made it attractive for its inclusion in this study. A technical specification from the manufacturer is attached in Appendix A.

3.3 Illinois Flexibility Index Test (I-FIT)

The Illinois Flexibility Index Test (I-FIT) was developed by researchers at the Illinois Center for Transportation (ICT) at the University of Illinois at Urbana–Champaign as a scientific and practical fracture test capable of screening AC mixes for cracking potential based on an index based on fracture mechanics principles *(63)*.

The test is in accordance of AASHTO TP124 protocol *(89)*, and consists of fabricating a semi-circular specimen with a central notch on its base, mount it on roller supports and loading it from the top by applying a monotonic displacement rate of 50 mm/min. The test stops once the recording load gets to 10% of the peak load. Table 3.3 shows the test parameters and Figure 3.4 presents the primary outputs from the test, respectively. The secant modulus value indicates the stiffness of the material before crack propagation and is defined as the ratio between 50% of peak load and the displacement at that point. Flexibility Index (FI) can be obtained using Equation 1. In general, higher values of FI indicate higher resistance to cracking propagation.

$$FI = A * \frac{G_f}{abs(m)} \quad (1)$$

where:

FI = flexibility index

G_f = fracture energy, defined as the area under the load-displacement curve (J/m^2)

m = slope of the tangent obtained at the inflection point of the post-peak curve (kN/mm)

A = unit conversion and scaling coefficient, taken as 0.01.

Table 3.3 Specimen and test parameters for I-FIT test

I-FIT Parameters	
Specimen Thickness (mm)	50 ± 1
Specimen Diameter (mm)	150 ± 1
Notch Length (mm)	15 ± 1
Notch Width (mm)	1.5 ± 0.05
Loading Rate (mm/min)	50
Test Temperature (°C)	25

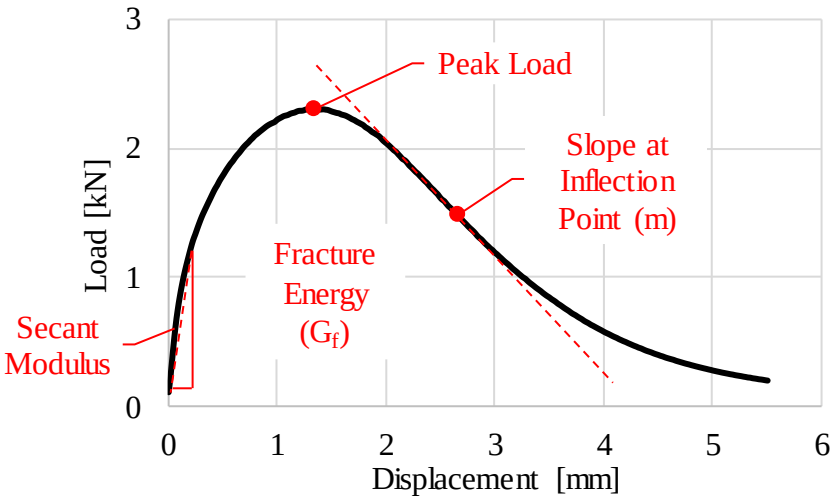

Figure 3.4 Typical outcome from I-FIT test, after Ozer et al. *(63)*

3.4 Hamburg Wheel Track Test (HWTT)

Hamburg Wheel Track Test is a standard test to evaluate the permanent deformation susceptibility of AC mixes. The HWTT is performed in accordance with AASHTO specification T324 *(90)*. The test subjects two pairs of AC samples, with 150 mm in diameter and 62 mm in thickness, to a cyclical loading from a rolling-wheel device; while tested specimens are submerged in a 50 °C

water bath. A total of 2 sets, each consisting of 2 pills, were tested for each conditioning combination. Figure 3.5 shows an example of the HWTT output and its main components.

The objective of the test is to measure the depression (in mm) formed on the specimens after a predefined number of passes or to record the number of passes that were necessary to achieve a predefined maximum depression level. Lower depression measurements, or the higher number of passes, are indicators that the mix is more rutting resistant. AASHTO T324 also indicates that as part of the HWTT output it is possible to obtain the Stripping Inflection Point (SIP), which may be used as a parameter to discriminate the moisture susceptibility of the mix. SIP is measured at the intersection of the 'Creep Slope' and 'Stripping Slope'; which are obtained by linear interpolation within the linear sections of the 'Creep Phase' and 'Stripping Phase', respectively. SIP is reported as the number of passes at the intersection point and can be obtained using Equation 2. Higher values of SIP indicate less moisture susceptibility of the test material.

$$SIP = \frac{intercept(stripping\ phase) - intercept(creep\ phase)}{slope(creep\ phase) - slope(stripping\ phase)} \quad (2)$$

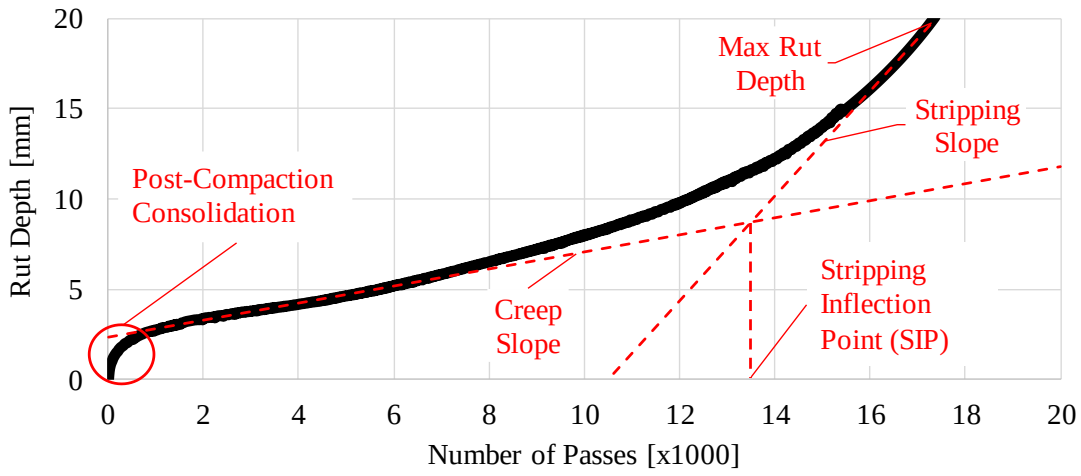

Figure 3.5 Typical outcome HWTT

3.5 Balance Mix Design

Researchers at the ICT at the University of Illinois at Urbana–Champaign has applied the concept of Illinois Balanced Mix Design (I-BMD) to improve the screening of high and low-performance AC mixes *(63, 91, 92)*. Their approach consists of analyzing two types of interaction plots, a 2-D plot between FI and rut depth, and a 3-D plot combining FI, rut depth, and secant modulus. Both 2-D and 3-D plots combine results from I-FIT and HWTT into four performance quadrants, while values are checked against secant modulus threshold as a check for mixture stiffness in the 3-D plot. The inclusion of secant modulus is recommended as it has been found to be an adequate proxy for mixture stiffness, and it does not require additional testing since it is readily available from I-FIT data *(92)*. The performance quadrants are defined as:

QI. Stiff and flexible: mixes with adequate cracking (flexible) and rutting (stiff) resistance.

QII. Soft and flexible: mixes with good crack resistant (flexible) but high rutting potential (soft).

QIII. Stiff and brittle: low rutting potential (stiff) but prone to cracking (brittle).

QIV. Soft and unstable: low cracking and rutting resistance.

The secant modulus range was selected to be between 2 and 10 kN/mm (11.4 to 57.2 kip/in). For FI, a minimum of 8 was considered acceptable, but, for high-performance mixes such as SMA, a minimum FI of 10 was taken as the minimum threshold. The maximum acceptable rut depth is 12.5 mm at 10,000 passes for the N50, and for the SMA mixes, the maximum rut depth allowed was taken at 7.5 mm at 20,000 passes. The quadrants' definitions and thresholds are based on previous work carried at ICT *(61–63, 91, 92)*. It is important to notice that threshold levels should be adjusted for local materials and conditions.

CHAPTER 4: TESTS RESULTS, ANALYSIS, AND DISCUSSION

4.1 SMA Performance

This section presents the results from the experimental testing performed on the COOEE SMA materials. These mixes showed remarkably high FI values, small rut depths after 20,000 passes from HWTT, and little to no moisture susceptibility based on SIP values. However, only SMA6 COOEE falls within the proposed secant modulus range of 2 to 10 kN.

4.1.1 Binder Grading

Table 4.1 summarizes the results obtained from the PG grading test for the binder samples. The final PG grade for the PEN 70/100 binder was PG64-28 (S), and for the PMB 40/100-75 PG82-16 (S); "S" refers to "Standard Traffic" according to AASHTO classification. The PEN binder stiffness [S(t)], from BBR test, was above the allowed threshold of 300 MPa; however, the m-value parameter, which relates to the relaxation properties of the binder, was 13% above the minimum required value, an indication that the binder has excellent flexibility properties.

MSCR test results indicate that the polymer modified binder is more resistant to permanent deformation. The PG82-16 exhibits considerably lower non-recoverable compliance, 73.5% and 37.5% lower, at 0.1 and 3.2 kPa stress levels, respectively. Additionally, the %R, at both stress levels, for the modified binder was considerably higher than that for the unmodified binder. Higher recovery rates are expected for modified binders. Regarding stress sensitivity, both samples have a nonrecoverable stress difference, $J_{nr,\,diff}$, below the specified threshold of 75%; however, the PG64 has a lower $J_{nr,\,diff}$, compared to the PG82. This finding could be explained by the fact that the PG64

already experiences relatively high levels of nonrecoverable compliance at 0.1 kPa, with the difference between low and high-stress levels at only 10.5%. In both cases, J_{nr} is above 3.0 kPa^{-1}. By contrast, PG82 has a 42.4% difference, and in both cases, J_{nr} is well below 3.0 kPa^{-1}. The $J_{nr,\ 3.2}$, for both binders, is higher than 2.0 and lower than 4.5, which makes them fall within the classification of "Standard Traffic".

Table 4.1 PG grading test results

Test	PEN 70/100		PMB 40/100-75	
	Temp [°C]	**Result**	**Temp [°C]**	**Result**
DSR on Original[1] Binder				
Complex Shear Modulus, G [kPa]*	64	1.2	82	1.2
Phase Angle, δ [deg]	64	87.3	82	59.8
G / sin(δ) [>1.0 kPa]* †	64	1.2	82	1.4
DSR on RTFO[2] Residue				
Complex Shear Modulus, G [kPa]*	64	2.7	82	2.5
Phase Angle, δ [deg]	64	84.5	82	65.3
G / sin(δ) [>2.2 kPa]* †	64	2.7	82	2.7
DSR on PAV[3] Residue				
Complex Shear Modulus, G [kPa]*	22	4,470.8	37	305
Phase Angle, δ [deg]	22	53.1	37	43.3
G • sin(δ) [<5,000 kPa]* †	22	3,576.8	37	209
BBR on PAV Residue				
Stiffness, S(t) [<300 MPa] †	-18	325	-6	55.1
Slope, m-value [>0.300] †	-18	0.336	-6	0.302
MSCR on RTFO Residue				
J_{nr} at 0.1kPa, $J_{nr,0.1}$ [kPa^{-1}]	64	3.305	82	0.884
J_{nr} at 3.2kPa, $J_{nr,3.2}$ [kPa^{-1}]	64	3.651	82	2.284
Recovery at 0.1 kPa, $\%R_{0.1}$ [%]	64	2.5	82	59.6
Recovery at 3.2 kPa, $\%R_{3.2}$ [%]	64	0.6	82	21.4
Stress Sensitivity, $J_{nr,diff}$ [kPa^{-1}]	64	10.5	82	42.4

[1] Original: unaged binder, tested on parallel plate geometry: 25 mm diameter, 1 mm gap

[2] RTFO: Rolling Thin Film Oven, short-term aged binder, tested on parallel plate geometry: 25 mm diameter, 1 mm gap

[3] PAV: Pressurized Aging Vessel, long-term aged binder, tested on parallel plate geometry: 8 mm diameter, 2 mm gap. PAV aging is performed on RTFO aged binder samples.

† PG thresholds by ASTM D6373-16

4.1.2 I-FIT Performance

Figure 4.1 shows the average load-displacement curves obtained from the I-FIT test. The reference mix appears to be the first to experience fracture propagation since the location of the peak loads for both AV% levels occurs earlier in the displacement scale. For the COOEE mixes, SMA6 has greater peak load, and it occurs at lower displacement than that for SMA8. The change in AV% has an impact on the peak load achieved in the test; for both SMA8 Ref and SMA8 COOEE, the reduction in peak load due to increased AV% is on the range of 10%. In general, a lower peak load implies a strength reduction of the material; which may be validated by analyzing values of secant modulus presented in Table 4.2. Secant modulus values decrease when air voids are increased. The secant modulus values are higher for SMA8 Ref, followed by SMA6 COOEE, and SMA8 COOEE being the mix with the lowest values.

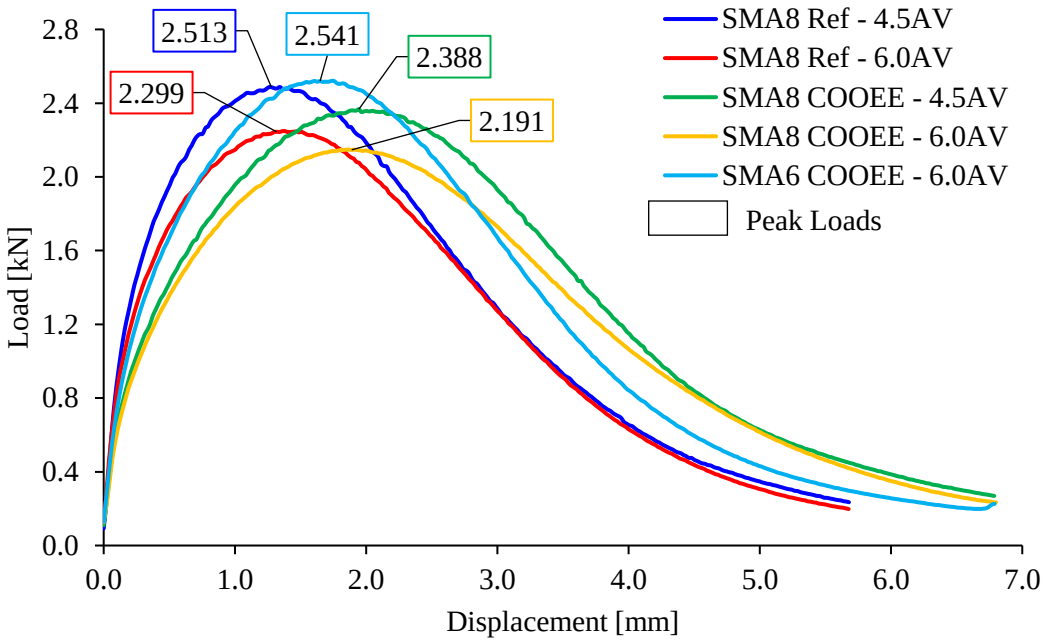

Figure 4.1 Average load-displacement curves for SMA

Table 4.2 summarizes the I-FIT output, including Coefficients of Variability (CoV). SMA8 COOEE showed the highest FI values regardless of AV% level. Compared to the reference material, SMA8 COOEE has higher binder and filler content, which improves the mastic quality; this translates into higher fracture-energy values and low slope values. The combination of these two effects, high fracture energy, and small slope, translates into higher FI values for SMA8 COOEE, indicating that this mix design is less susceptible to cracking. Compared to SMA6, SMA8 has a larger aggregate size, which could retard crack propagation. Since a crack propagates around larger size aggregate, it requires more time to travel through the particles, compared to the path around smaller size aggregate. This variable depends on the mix having tough and high-quality aggregate, as is the case for these mixes.

Table 4.2 Summary of I-FIT output

		Average					**CoV [%]**				
Mix	**Reps[1] [#]**	**Peak Load [kN]**	**Fracture Energy [J/m^2]**	**Secant Modulus [kN/mm]**	**Slope**	**FI**	**Peak Load [kN]**	**Fracture Energy [J/m^2]**	**Secant Modulus [kN/mm]**	**Slope**	**FI**
SMA8 Ref - 4.5AV	6	2.513	2774	3.00	0.942	30.4	21.1	15.9	20.8	20.1	23.9
SMA8 Ref - 6.0AV	15	2.299	2526	2.52	0.958	27.9	10.4	8.9	19.8	27.6	25.5
SMA8 COOEE - 4.5AV	8	2.388	3285	1.81	0.891	38.7	10.5	9.8	11.7	24.2	24.1
SMA8 COOEE - 6.0AV	13	2.191	2936	1.77	0.728	41.1	9.3	11.4	10.7	15.9	17.1
SMA6 COOEE - 6.0AV	9	2.541	3110	2.46	0.957	33.8	9.3	7.2	13.8	22.3	21.9

[1]**Reps:** number of replicates

All three mixes exhibited relatively high values of fracture energy and FI as compared to the results reported elsewhere *(63, 93)*, and to those of the results obtained from testing on the dense-graded mix, results which are presented in the next section. The prime factor influencing the high FI is the low slope values (< 1.000 for all mixes). The slope is an indicator of crack-propagation speed, and lower values indicate that the material is more resistant to crack propagation. The AV% level appears to have an impact on the different outputs of the I-FIT test, but without a clear trend, FI decreases with increasing AV% for SMA8 Ref, but FI increases with increasing AV% for SMA8 COOEE. The effect of AV% has been presented in other studies *(94, 95)*.

4.1.3 HWTT Performance

Figure 4.2 presents the progression of rut depth with increasing number of wheel passes for the three SMA. The best-performing mix was SMA6 COOEE, with only 3.6 mm rut depth after 20,000 passes. Mix SMA8 Ref exhibited the highest rut depth and showed significant sensitivity to increased air voids. There was a 65% increase in rut depth between the 4.5% and 6.0% AV% specimens, indication that the mix might be highly susceptible to post-compaction densification. Additionally, the linear 'Creep Phase' from SMA8 Ref appears to be considerably shorter at 6.0% AV%, and there was an evident presence of the perceived a 'Stripping Phase'. In contrast, SMA8 COOEE experienced only a 16% increase in rut depth, with increased AV%, from 4.4 to 5.1 mm.

It is important to notice that both COOEE mixes have a final rut depth, after 20,000 passes, below the maximum threshold of 7.5 mm. This threshold was established as a maximum for high-performance mixes based on previous research *(62)*. Also, both COOEE mixes did not exhibit a 'Stripping Phase', as the linear segment of the 'Creep Phase' for both mixes extended all the way

to 20,000 passes; which could be interpreted as another indicator of the high-performance nature of these mixes.

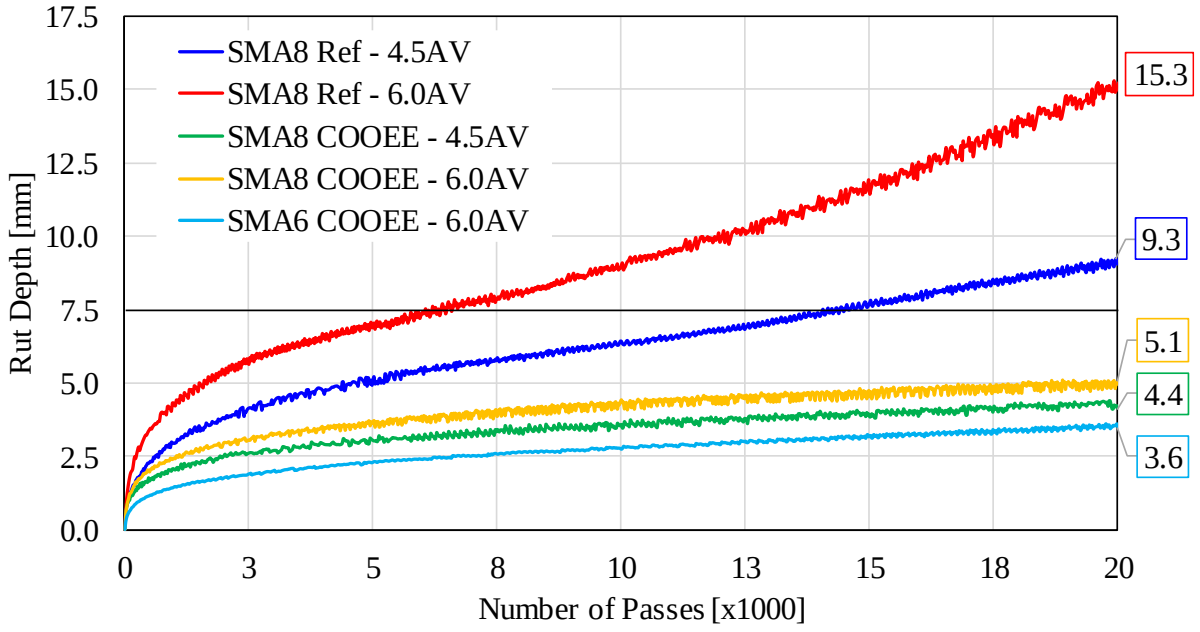

Figure 4.2 Rut-depth progression vs. Number of passes, 50°C test temperature

Regarding moisture damage, from Figure 4.2, neither of the COOEE mixes exhibited a potential stripping phase; thus, their respective SIP values are reported as greater than 20,000 passes. Lack of stripping phase in the HWTT does not imply that the COOEE mixes will be unaffected by moisture. Instead, it means that HWTT did not cause enough damage on the specimens to develop a stripping phase and subsequent failure, within specified limits of the test. Only SMA8 Ref at 6.0% AV% exhibited the initial stages of a potential stripping phase. The mix showed significant resistance as it did not present a sudden increase in rutting which could have led to specimen failure. Table 4.3 summarizes the moisture susceptibility analysis for the three SMA.

Table 4.3 Moisture susceptibility summary from HWTT output

	Creep Phase				Stripping Phase				
Mix Type	**Initial Pass**	**Ending Pass**	**Slope**	**Intercept**	**Initial Pass**	**Ending Pass**	**Slope**	**Intercept**	**SIP [# Passes]**
SMA8 Ref - 4.5AV	2,000	>20,000	N/A	N/A	>20,000	>20,000	N/A	N/A	>20,000
SMA8 Ref - 6.0AV	2,000	13,000	0.000434	4.72782	18,000	20,000	0.000662	1.90893	12,357
SMA8 COOEE - 4.5AV	2,000	>20,000	N/A	N/A	>20,000	>20,000	N/A	N/A	>20,000
SMA8 COOEE - 6.0AV	2,000	>20,000	N/A	N/A	>20,000	>20,000	N/A	N/A	>20,000
SMA6 COOEE - 6.0AV	2,000	>20,000	N/A	N/A	>20,000	>20,000	N/A	N/A	>20,000

The SIP value for SMA8 Ref – 6.0AV, was obtained by defining the stripping phase of the mix between 18,000 and 20,000 passes. However, the initial point of this phase was chosen arbitrarily by visually analyzing the data and deciding which was the most appropriate point that marked the beginning of the steady-state of the stripping phase. AASHTO T324 does not provide clear guidance on how to decide where does the steady-state for either the creep or stripping phases begins. The lack of guidance has been identified as a significant drawback for using HWTT to predict moisture susceptibility performance *(96–98)*. The lack of guidance can have a significant impact in the calculations of SIP values; case in point is SMA8 Ref – 6.0AV for which changing the beginning of the stripping phase from 18,000 to 17,000 passes its SIP value changes from 12,357 to 13,286, a 7.5% difference.

4.1.4 I-BMD Analysis

Figure 4.3 presents the interaction plot for all the AC mixes in this study. The thresholds for the 2-D I-BMD analysis were based on the high-performance limits discussed in Chapter 3; a minimum FI of 10, and a maximum rut depth of 7.5 mm at 20,000 passes. It is evident that both COOEE mixes have significantly high FI values, higher than what is usually experienced with AC mixes in the United States. This finding could be explained by the higher amount of asphalt content, modified binder, and high-quality filler that results in a rich mastic. Also, these mixes exhibited low rut depth, as is expected for SMA designs. These two factors, made the COOEE mixes to be classified as stiff and flexible, regardless of AV%. The combination of high flexibility, low rutting potential, and low moisture susceptibility, indicate that both types of COOEE mixes could exhibit better durability in the field if produced and constructed adequately.

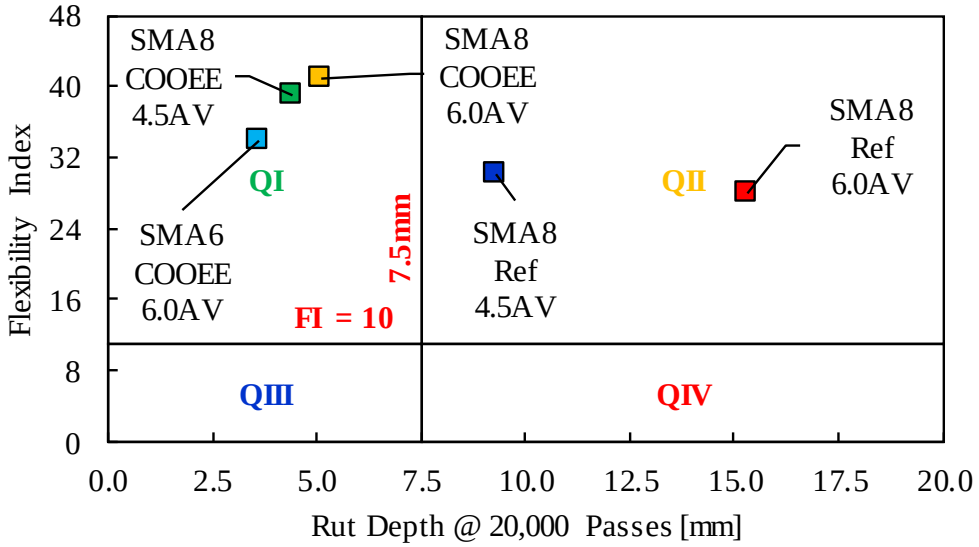

Figure 4.3 FI and rut depth interaction plot for SMA

Figure 4.4 shows the expanded 3-D I-BMD plot by adding the secant modulus criterion. In this plot, a red color indicates that the data point failed either FI or rutting, yellow color indicates data points that passed both FI and rutting but have secant modulus value outside the range; blue color indicates compliance with the three criteria. The light-green shaded borders represent the threshold limits for QI, the rest of the quadrants are not explicitly delimited to avoid overcrowdedness. SMA8 COOEE, which showed the highest flexibility values, fell outside the proposed range of 2 to 10 kN/mm, indicating that the high FI values obtained are due to a relatively softer mix. Adding secant modulus as a third performance criterion is recommended since it does not require additional testing, the data is available from the I-FIT test output, and its inclusion could identify potentially overly soft or stiff mixes *(92)*.

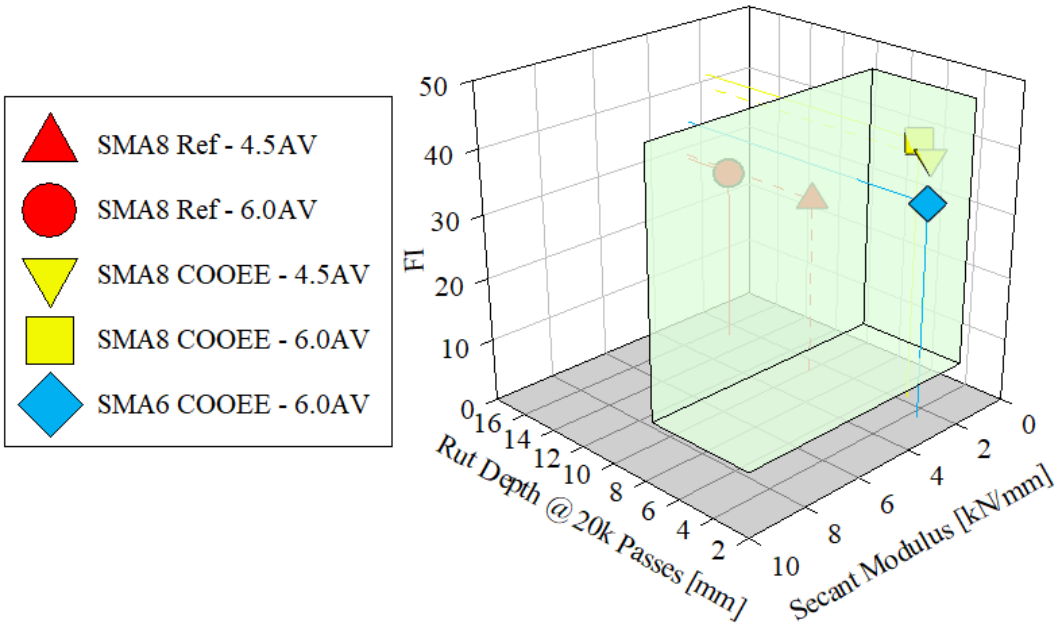

Figure 4.4 3-D I-BMD interaction plot SMA mixes

4.2 Rejuvenation and Aging Effects

This section presents the results from the experimental testing performed on the N50 mix. Adding rejuvenator to the N50 mix showed that it positively affects flexibility, and negatively impacts rutting resistance. The increasing effect on flexibility becomes less relevant with increasing dosages; but, for rutting, it becomes more dominant. The short-term aging condition appears to have a more substantial influence on rutting resistance than on flexibility.

4.2.1 I-FIT Performance

Figures 4.5 and 4.6 show the load-displacement curves for the UA and STA samples. The reduction of peak-load magnitudes and an overall flattening of the post-peak curves is a clear indication that higher dosages of rejuvenator induced a stronger softening effect on the material. The softening effect can be interpreted as the overall decrease in stiffness of the material, which can be seen in the decreasing peak loads and flattening slopes of the post-peak part of the curves. In absolute terms, UA blends experienced a 53% drop in peak-load magnitude between the control mix (0% rejuvenator) and the 9% blend; STA blends experienced a 46% between the same two conditions.

Table 4.4 summarizes the primary results from I-FIT along with their respective CoV. Regarding fracture energy, there is no consistent trend concerning increased rejuvenator dosage. Fracture energy values go up from 0% to 3% but then experience an overall decrease in both UA and STA conditions; this could indicate that fracture energy alone may not be a suitable parameter to differentiate between AC mixes as has been shown by previous research *(61, 63, 95, 99)*.

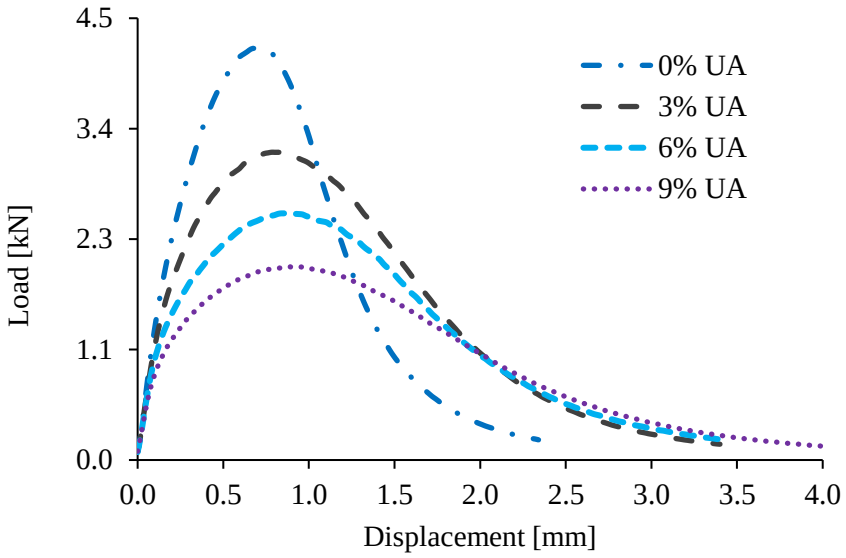

Figure 4.5 Load-displacement curves for UA samples

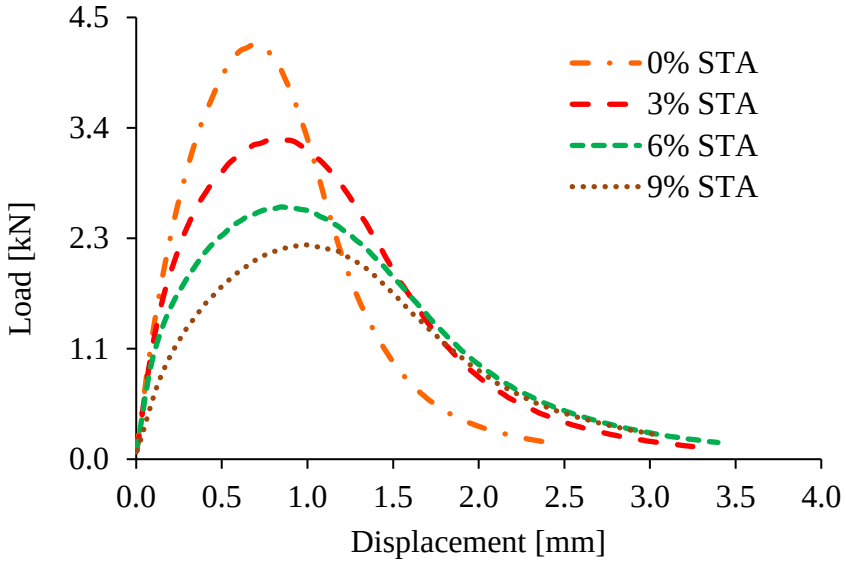

Figure 4.6 Load-displacement curves for STA samples

As explained in the discussion of the SMA results, the slope value is a term derived from the load-displacement curve defined at the inflection point of the post-peak slope, and it is included in the FI calculation since it was found that it closely correlates to crack growth speed *(63)*. Therefore,

higher absolute slope values indicate an AC mix that experiences faster crack propagation, while lower values are related to slower crack propagation. Table 4.4 shows that with increasing rejuvenator application there is a reduction in slope values, with the steepest decline happening between 0% and 3%. Regarding the effect of STA, there is an increase in slope values, with the highest relative difference between conditions presented on the specimens with 9% rejuvenator, with a difference close to 42%.

Table 4.4 Output from I-FIT test, R = Rejuvenator

			Average					CoV [%]				
Blend	**Condition**	**Reps[1] [#]**	**Peak Load [kN]**	**Fracture Energy [J/m2]**	**Secant Modulus [kN/mm]**	**Slope**	**FI**	**Peak Load [kN]**	**Fracture Energy [J/m2]**	**Secant Modulus [kN/mm]**	**Slope**	**FI**
0% R (Control)	**UA**	18	4.27	1602	9.37	5.56	3.0	4.6	9.7	13.0	15.0	20.3
	STA	14	4.32	1558	9.49	5.59	2.9	4.4	5.9	15.9	17.9	18.9
3% R	**UA**	10	3.20	1838	6.12	2.42	7.9	7.3	7.2	22.0	19.5	20.6
	STA	14	3.30	1710	6.67	2.89	6.0	5.8	6.7	15.0	12.2	16.4
6% R	**UA**	10	2.53	1701	4.60	1.78	9.9	10.9	14.3	11.4	15.7	25.3
	STA	14	2.59	1586	4.69	2.00	8.4	13.2	9.7	18.9	23.2	30.7
9% R	**UA**	12	1.99	1389	3.50	1.17	12.0	6.4	8.9	10.6	13.4	13.8
	STA	15	2.34	1593	3.90	1.65	10.7	17.5	13.7	25.3	41.8	30.8

[1]**Reps:** number of replicates

FI is obtained by combining the values of fracture energy and slope. In this case, there is an overall trend of increasing FI with higher rejuvenator dosages; this reflects the effectiveness of using a rejuvenator to improve the potential cracking resistance of AC. The most significant jump in FI is experienced between 0% and 3% specimens, and as higher dosages are used, the FI improvement becomes of less relative impact. Although the CoV for FI is greater than fracture energy, the ability of FI to discriminate the effect of the rejuvenator content and aging is evident.

4.2.2 HWTT Performance

Figures 4.7 and 4.8 show the rut depth progression against the number of passes for UA and STA samples, respectively. Evaluating the entire span of the test, both types of conditioning show higher values of rut depth with increasing levels of rejuvenation; this effect was more pronounced for UA samples. At the lowest concentration of 3% rejuvenator, there was a significant increase in rut depth progression compared to the control blend, and after 20,000 passes it was barely above the maximum threshold of 12.5 mm. On the other hand, for the STA samples, only at 9% rejuvenator concentration a severe rutting deterioration occurred. It should be expected that adding rejuvenator to the AC mix would reduce its permanent deformation resistance since the rejuvenator softens the asphalt binder in the mix.

STA conditioning reduced the rutting experienced by the different blends, judging from the extended steady-state portion of the creep phase. For the blends with 3% and 6% rejuvenator, this effect was strong enough that the blends switched from having an evident stripping phase in the UA condition to not exhibiting stripping under STA condition. Additionally, the stiffening that the binder-rejuvenator blend sustained during STA made the post-compaction consolidation phase of the mixes less significant. For UA conditions post-consolidation induced a rut depression close to 2.5 mm, whereas for STA condition the consolidation experienced was only of the magnitude of 1.8 mm, about half of that from UA specimens.

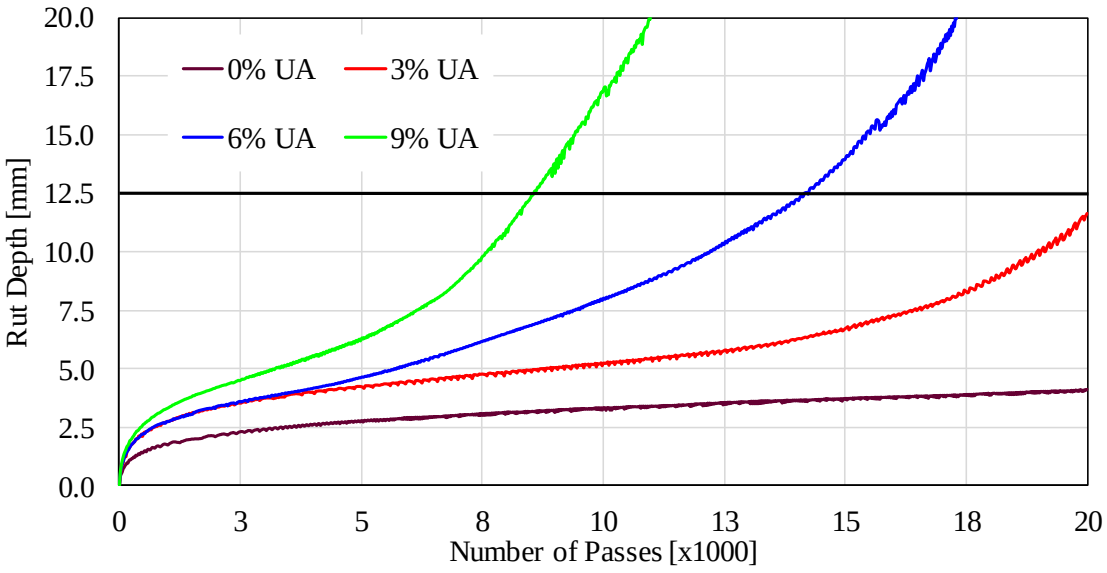

Figure 4.7 Rut-depth progression for UA samples

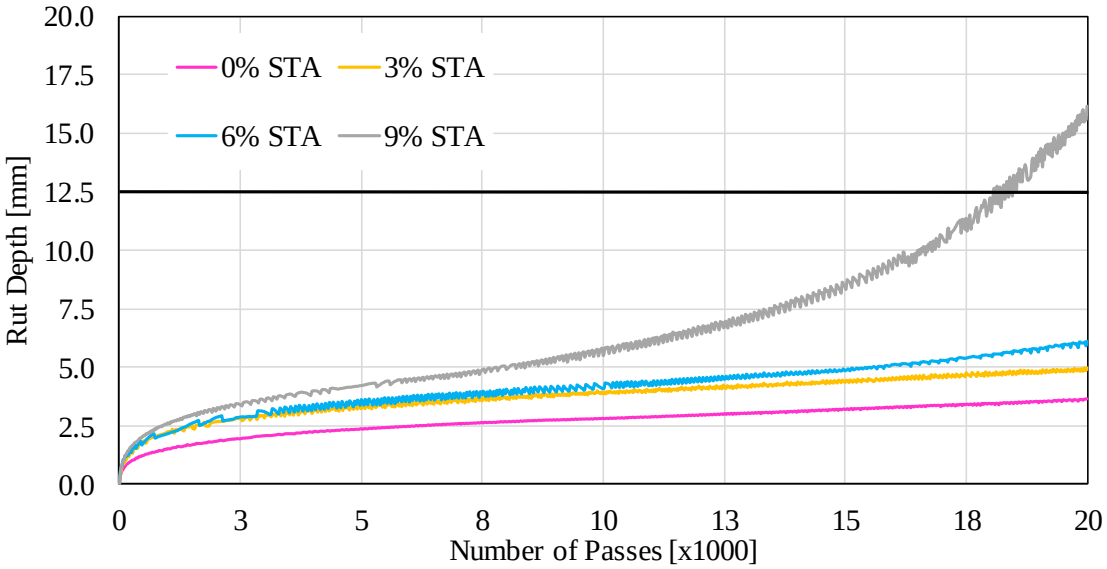

Figure 4.8 Rut-depth progression for STA samples

Mix N50 is blended with a PG 64-22; in Illinois, the pass/fail criterion for rut depth for AC mixes prepared with this binder grade is compared to the maximum allowed threshold of 12.5 mm at 7,500 passes. However, at that point, all samples were above it. Thus, a comparison of final rut depth was

performed at 10,000 passes since there was rut progression data available for all blends, and at this point, the effect of any potential stripping presence would be more apparent. Figure 4.9 presents the rut depth after 10,000 passes for all AC blend types. The plot shows a direct relationship between increasing dosage and rut depth; with a significant increase when 9% rejuvenator was added. On the other hand, STA samples showed a much smaller and constant increment between the different concentration levels, which could be related to the steady-state creep phase extension that STA appears to have induced in the blends.

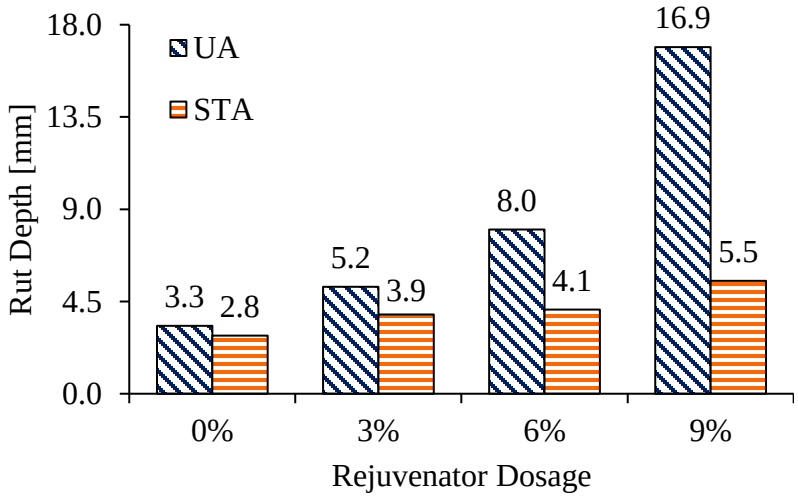

Figure 4.9 Final rut depth at 10,000 passes, all blends

Regarding moisture damage, it was possible to observe from Figures 4.7 and 4.8 that the control blend did not experience a stripping phase, within the limits of the test, regardless of aging condition. Thus their SIP values were reported as greater than 20,000. For the rejuvenated blends, it was discussed that with increasing dosage the binder becomes softer inducing higher rutting in the AC mix. Additionally, higher dosages propitiated the appearance of a potential stripping phase on all UA blends, with increasing potential of stripping severity with increasing dosage; this is

evident on the decreasing magnitude of their respective SIP values, ranging from 17,079 for the 3% blend to 7,070 to the 9% blend. Short-term aging mitigated the softening impact of the rejuvenator, to the point that only the 9% blend continued to experience a stripping phase during the test, but even then, the SIP value reported is on the further side of the scale, at 15,450. Table 4.5 summarizes the result of the stripping point analysis.

Table 4.5 Moisture susceptibility for N50 samples

	Creep Phase				Stripping Phase				
Mix Type	**Initial Pass**	**Ending Pass**	**Slope**	**Intercept**	**Initial Pass**	**Ending Pass**	**Slope**	**Intercept**	**SIP [# Passes]**
0% UA	2,000	>20,000	N/A	N/A	>20,000	>20,000	N/A	N/A	>20,000
0% STA	2,000	>20,000	N/A	N/A	>20,000	>20,000	N/A	N/A	>20,000
3% UA	2,000	12,000	0.000213	3.11051	19,000	20,000	0.001622	-20.9545	17,079
3% STA	2,000	>20,000	N/A	N/A	>20,000	>20,000	N/A	N/A	>20,000
6% UA	1,000	7,000	0.000470	2.36357	16,000	17,000	0.003026	-32.5499	13,658
6% STA	2,000	>20,000	N/A	N/A	>20,000	>20,000	N/A	N/A	>20,000
9% UA	1,000	5,000	0.000695	2.76074	9,000	11,000	0.003109	-14.3122	7,070
9% STA	2,000	8,000	0.000279	2.78740	18,000	20,000	0.001802	-20.3545	15,450

4.2.3 I-BMD Analysis

Figure 4.10 presents the 2-D interaction plot for all AC mixes in this study, and Figure 4.11 shows the expanded 3-D interaction plot integrating secant modulus. The color scheme for the 3-D plot is the same as the one described in section 4.1.4 regarding Fig. 4.4.

In the 2-D diagram, both control AC mixes, aged and unaged, fell within the undesirable quadrant QIII, stiff and brittle. As the rejuvenator dosage increased, the AC mix became more flexible, it

achieved higher FI values, but at 9% this softening effect was so excessive that mix becomes undesirably soft. From the 3-D plot, the secant modulus decreased with increasing rejuvenator dosage, but it appears to be the least sensitive variable to it. It is evident that the use of the rejuvenator, and aging condition, impact the location of the AC mix on the I-BMD plot.

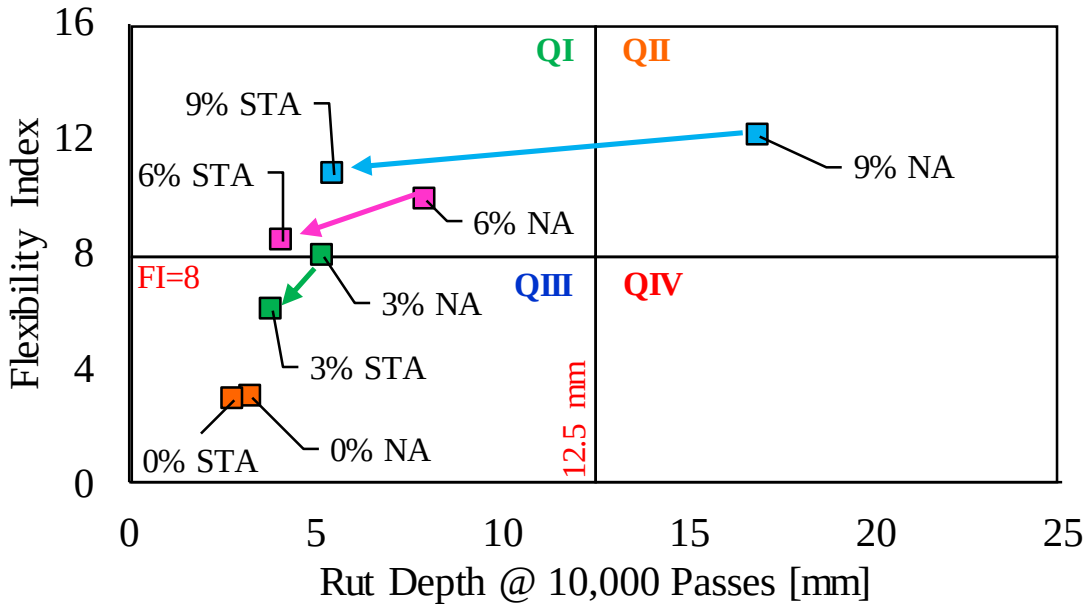

Figure 4.10 2-D Interaction plot between rut depth and FI

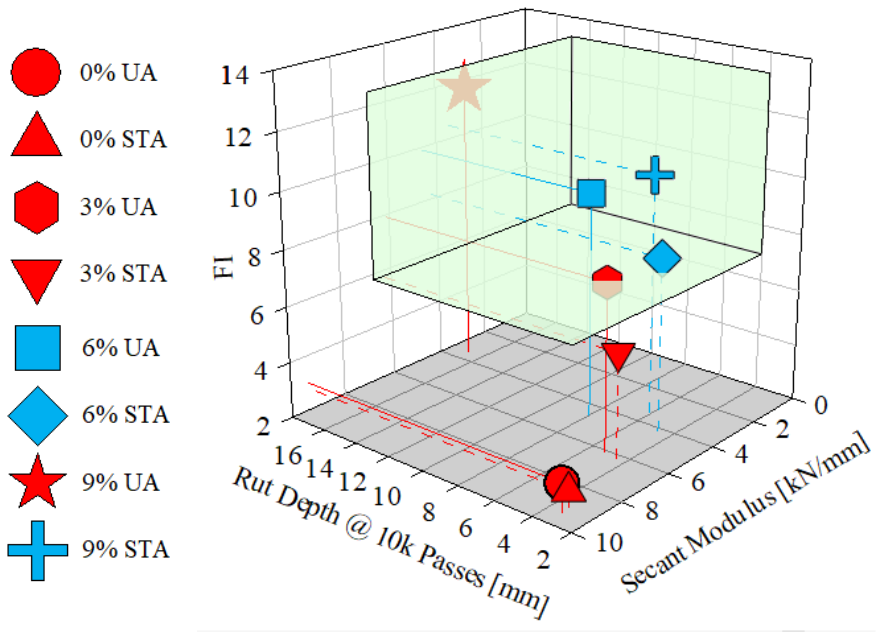

Figure 4.11 3-D Interaction plot between rut depth, FI, and secant modulus

Aging showed that it reduces flexibility and rutting potential, but this effect is not proportional to each property. At 9% dosage, the STA samples switched from being above the 12.5 mm rutting threshold to being below it, by experiencing a 67% reduction in the final rut depth at 10,000 passes, from 16.9 to 5.5 mm. However, the reduction in FI between 9% UA, and 9% STA amounts only to an 11% drop; highlighting how adding rejuvenator to an AC mix could improve its durability regarding cracking resistance, without suffering significant reductions in rutting resistance, if the aging condition is considered. Similar high drops in final rut depth and relatively smaller drops in FI, between UA and STA samples, were observed for the other rejuvenated dosages, as shown in Table 4.6. Secant modulus increased between the two conditions, but the effect was less evident. Ultimately, an optimum rejuvenator dosage could be obtained to provide a durable AC mix; for the case of the N50 mix, the most appropriate dosage appeared to be 6% since both UA and STA samples fall to comply with the three criteria.

Table 4.6 Changes in I-BMD criteria between UA and STA samples, all dosages

Mix Type	FI	Rut @ 10,000 Passes [mm]	S_{mod}[1] [kN/mm]	Δ% FI (decrease)	Δ% Rut (decrease)	Δ% S_{mod} (increase)
0% UA	3.0	3.3	9.4	3.3%	15.2%	1.3%
0% STA	2.9	2.8	9.5			
3% UA	7.9	5.2	6.1	24.1%	25.0%	9.0%
3% STA	6.0	3.9	6.7			
6% UA	9.9	8.0	4.6	15.2%	48.8%	2.0%
6% STA	8.4	4.1	4.7			
9% UA	12.0	16.9	3.5	10.8%	67.5%	11.4%
9% STA	10.7	5.5	3.9			

[1] **S_{mod}**: Secant Modulus

4.3 Combined I-BMD Analysis

From the analysis and discussion presented in this Chapter, it is clear that the SMA materials from the Danish Road Directorate exhibited superior performance regarding potential cracking and permanent deformation resistance, along with low moisture damage susceptibility; these characteristics highlight their high durability potential. Alternatively, a commonly used dense-graded mix (N50) from the mid-Illinois region presented low FI values in its original condition, suggesting weak cracking resistance. However, the N50 mix presented little rutting and no indication of moisture damage during the HWTT.

By adding an adequate amount rejuvenator to the N50 mix, it was demonstrated that it is possible to improve the cracking resistance characteristics of the mix, without overly damaging its permanent deformation and moisture damage resistance characteristics. In this context, it was of interest to carry a performance comparison between the various N50 blends against the different types of SMA. The performance comparison was achieved by combining the data from both types of mixes into an expanded 2-D I-BMD diagram. Ten thousand passes were selected as the analysis point for rut depth to be consistent with the criterion used for the N50 analysis.

Figure 4.12 presents the expanded 2-D I-BMD diagram incorporating the thresholds used for regular mixes to define the four quadrants (FI = 8, Rut = 12.5 mm) and adding a 'High-Performance' sub-quadrant (QI-HP) within QI using more stringent criteria (FI = 10, Rut = 7.5 mm). Also, the secant modulus criterion is incorporated using a color scheme. Red indicates a failure in FI or rut depth. Yellow points are compliant with FI and rut depth, but secant modulus is outside the desired range. Green means compliance with all three criteria and location within QI.

Blue also indicates conformity with all the criteria, but the location is within the most desirable QI-HP.

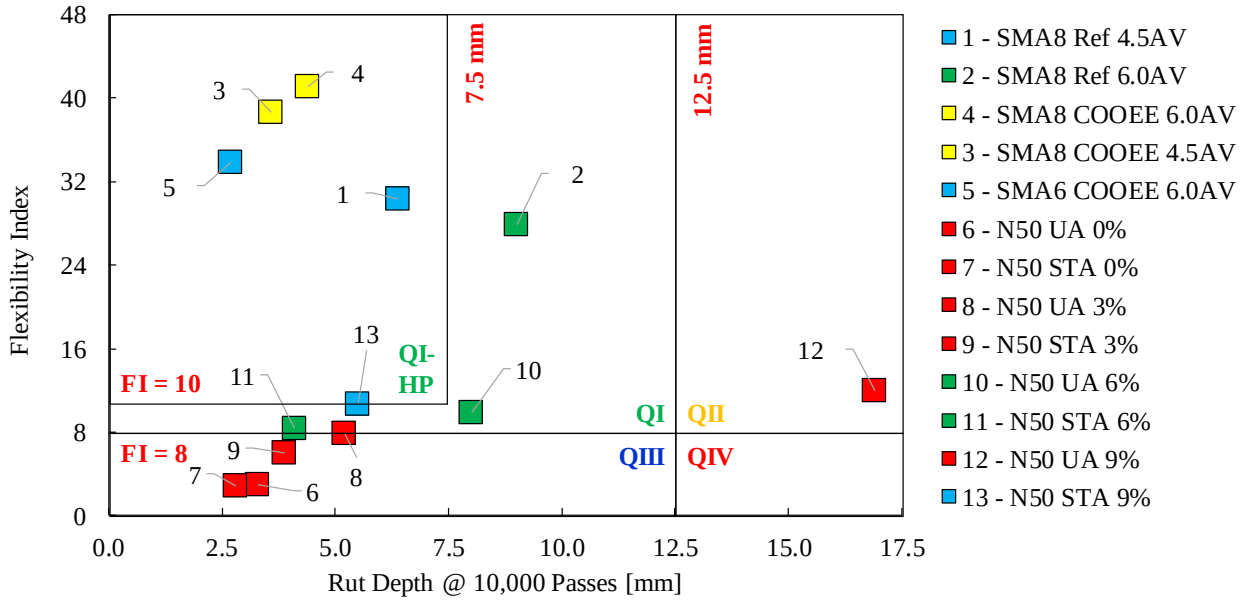

Figure 4.12 Expanded 2-D I-BMD diagram, comparing SMA mixes and N50 blends

From Figure 4.12, the significant difference in flexibility between the SMA and N50 is evident; there is at least a twofold spread between FI values. Regarding permanent deformation, except for N50 UA 9%, the final rut depths are relatively similar. Regarding the effect of rejuvenation, as mentioned earlier, it improves flexibility performance without excessively affecting rutting resistance in most cases. However, the flexibility improvement was limited compared to the high-performing SMA. The FI values for N50 are only capable of reaching the QI-HP boundary of 10 when 9% rejuvenator is added; but at this point, the softening effect induced by such a high dosage severely affects the rutting and moisture resistance of the mix.

Regarding moisture damage susceptibility, it was found that only one type of SMA and four N50 blends experienced a potential stripping phase, therefore SIP values were only obtained for these materials. Figure 4.13 shows the materials that possibly have potential stripping and their respective SIP values. Interestingly, this comparison suggests that the second worst mix, concerning potential moisture damage, is SMA8 Ref – 6.0AV; however, this might be a counterintuitive assessment from the rut progression curves presented in Figure 4.14.

The progression curves show that the different N50 blends have a clear stripping phase; they show a clear distinction between the steady-state creep phase and the increased rate of change for the rut depth afterward. On the other hand, the appearance of the stripping phase for SMA8 Ref – 6.0AV is less clear, and it would seem that the rate of change of rut depth in this region for the SMA is not as rapid as for the N50 blends.

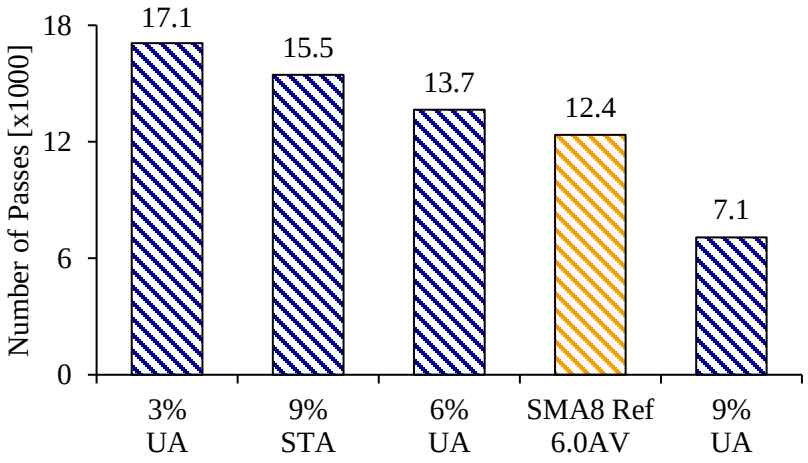

Figure 4.13 SIP values for mixes exhibiting 'Stripping Phase'

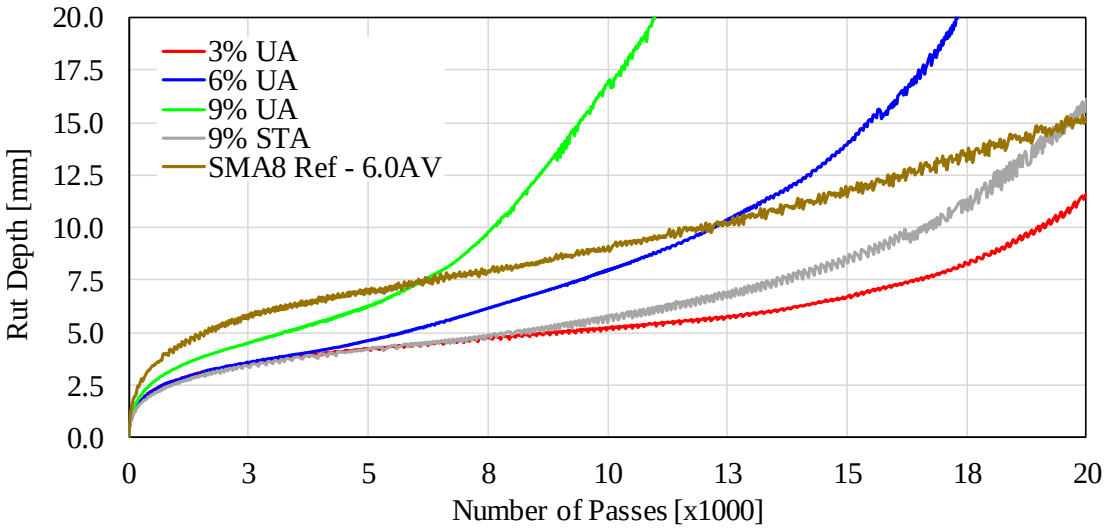

Figure 4.14 Rut depth progression curves for mixes exhibiting potential 'Stripping Phase'

During the discussion regarding the HWTT performance of the SMA, it was mentioned that one significant disadvantage of using HWTT data to predict moisture damage susceptibility was the arbitrary related to deciding where do the creep and stripping phases start and end; which could lead to significant differences in SIP values. To reduce the uncertainty involving SIP values a more objective approach could be to identify the point at which the curvature of the rut progression line changes from negative to positive, in essence, identify the inflection point of the curve.

An adequate mathematical model that describes the rut depth relation with the number of passes is needed to calculate the inflection point of the curve. Different agencies have used high-order polynomials as fitting models. However, it has been documented that this approach might not capture local trends especially at the end of the progression curve *(98)*. Alternatively, researchers in Texas have employed a non-linear model to describe the rut progression data and used different model parameters as indicators of the rutting and moisture resistance of AC *(96)*.

To improve comparison accuracy between for SMA8 Ref – 6.0AV and the N50 blends, the method described by Yin et al. *(96)* was adopted to evaluate the moisture susceptibility of the AC mixes presenting a stripping stage; their model to described rut depth progression is defined by Equation 3. The proposed method introduces a stripping number (SN) parameter that indicates where the stripping phase initiates; SN is found at the inflection point of the second derivative of Equation 3. The expression for SN is described by Equation 4. Similarly to SIP, higher SN values imply less potential moisture damage susceptibility of the material.

$$RD_{LC} = \rho * \left[\ln\left(\frac{LC_{ult}}{LC}\right)\right]^{-\frac{1}{\beta}} \quad (3)$$

where:

RD_{LC} = rut depth at a certain number of load passes (mm)

LC = number of load passes

LC_{ult}, ρ, and β = model coefficients

$$SN = LC_{ult} * \exp\left(-\frac{\beta+1}{\beta}\right) \quad (4)$$

where:

SN = stripping number (# passes)

LC_{ult}, and β = model coefficients from Equation 3

Figure 4.15 display the final SN values obtained for the AC mixes presenting potential stripping. Contrary to what was concluded from analyzing only the SIP values in Figure 4.13, the SN trend shows that SMA8 Ref – 6.0AV has much better moisture resistance characteristics than the N50 blends. The change in conclusion, caused by changing the analysis approach, goes more in line with

the characteristic of the SMA since it contains more binder content and fewer air voids than the N50 mix.

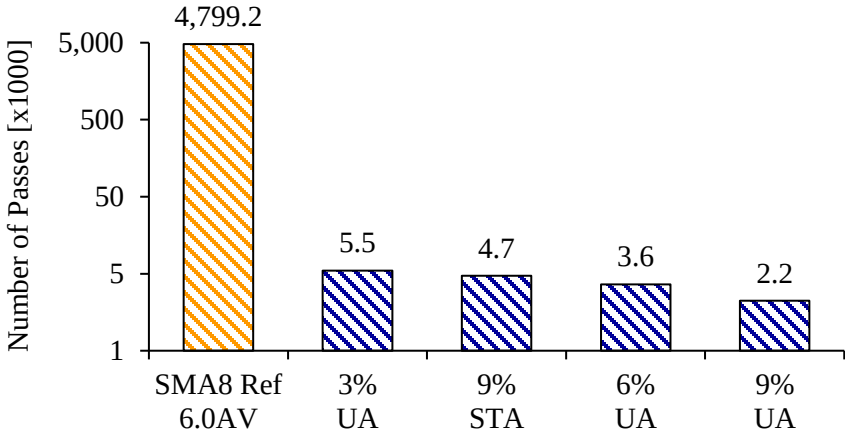

Figure 4.15 SN values for mixes that exhibit a potential 'Stripping Phase'

The model fitting was performed by minimizing the sum of the squares of the errors using the SOLVER tool from Microsoft Excel®. Table 4.7 presents the model coefficients for Equation 3 together with R^2-values as a goodness-of-fit parameter, and the final SN, for the different AC mixes that exhibit a potential stripping phase.

Table 4.7 Fitting results for Equations 4 and 5

Mix Type	LC_{ult}	ρ	β	R^2	SN [# Passes]
SMA8 Ref 6.0AV	6.99E+08	1,320,860	0.251166	0.9911	4,799,205
3% UA	22,114	4.7063	2.553648	0.9929	5,499
6% UA	22,714	6.7280	1.202122	0.9995	3,637
9% UA	14,809	7.1036	1.123200	0.9941	2,236
9% STA	23,105	5.2220	1.695884	0.9961	4,713

CHAPTER 5: SUMMARY, FINDINGS, CONCLUSIONS, AND RECOMMENDATIONS

5.1 Summary

Limited financial resources, reduced availability of raw materials, and environmental concerns have renewed the interest in improving the durability of AC pavements. It has been well documented that high-performance mixes such as SMA may improve the overall durability of flexible pavements. However, cost and strict material requirements to design high-performance AC mixes could be prohibitive for most paving projects. Therefore, it is necessary to improve AC durability for conventional designs, such as dense-graded mixes. This study presents the performance results from I-FIT and HWTT, and their implications for durability, for novel types of SMA, designed by the DRD, and for a conventional Illinois dense-graded mix blended with various dosages of rejuvenator to enhance its characteristics. The findings, conclusions, and recommendations of this study are presented in this Chapter.

5.2 Findings

The study resulted in the following findings on the durability assessment of the SMA provided by the DRD:

- The COOEE mixes are distinguished by the strong, polymer-modified binder, high asphalt content, and the type and amount of filler used. Binders used in the new mixes were graded as PG82-16 (S) as compared to PG64-28 (S) used in reference mix (SMA Ref).

- COOEE mixes exhibited exceptionally high FI values, suggesting low cracking susceptibility. Also, both mixes suffered low rut depths after 20,000 passes of HWTT, compared to SMA Ref; indicating a strong permanent-deformation resistance.
- None of the COOEE type mixes showed evidence of potential moisture damage susceptibility within the constraints of the HWTT. Only SMA8 Ref at 6% air voids developed the initial stages of a stripping phase.
- Except for SMA8 Ref – 6.0AV, a change in compaction density did not appear to influence the performance of any of the SMA materials significantly.
- On an I-BMD analysis, both COOEE materials were classified as stiff and flexible; underscoring their high-performance potential. However, when adding a stiffness criterion using secant modulus, only SMA6 COOEE fell within the boundaries of all three parameters.

The following findings were observed for the analysis of the dense-graded mix (N50) when it was blended with different dosages of rejuvenator, and subjected to short-term aging:

- The original mix (control), returned low values of FI, close to 3, suggesting that using this mix could jeopardize pavement durability regarding cracking distresses.
- Adding a rejuvenator increased the FI values of N50, which is a positive effect. The rate of increase, however, was not constant and its influence diminished as the dosage increased.
- Secant modulus was reduced with increasing dosage of rejuvenator, but this effect was small compared to the other variables.
- On the other hand, higher rejuvenator dosages negatively affected rutting resistance, and this effect continued to grow as the amount of rejuvenator was increased.

- Regarding potential moisture damage susceptibility, increasing amounts of rejuvenator diminished the potential stripping resistance of the AC mixes. While the control mix only presented a steady-state creep phase, with increasing dosage, the mix quickly developed a stripping phase.
- FI values of the AC mixed decreased with simulated short-term aging conditions, slightly increased secant modulus, and improved rutting and potential moisture resistance. The most sensitive variable was rutting.

From performing a combined analysis of the SMA and N50 materials, the following findings were noted:

- Increasing the amount of rejuvenator dosage did improve the performance the of the N50 mix, and at 6% it fell within the desirable QI quadrant on an expanded 2-D I-BMD diagram; however, the flexibility gains were not enough to get into the best QI-HP quadrant, which is where the SMA materials were located.
- Regarding potential moisture resistance, the initial assessment based on interpreting SIP values for the mixes that exhibited a stripping phase showed that the SMA8 Ref – 6.0AV was the second mix type, only in front of the N50 9% UA.
- By applying a model fitting method to assess moisture susceptibility, it was found that the SMA8 Ref – 6.0AV had better moisture resistance since its SN value was three orders of magnitude higher than those of the different N50 blends.

5.3 Conclusions

Based on the discussion and findings presented in this study, the following conclusions are made:

- SMA showed performed well against potential rutting and crack propagation; indicating that pavements constructed with these materials should exhibit superior durability since low cracking and permanent-deformation distresses would be expected. Additionally, there is little indication that the mixes would have potential moisture damage.
- Applying the I-BMD approach on a 2-D and 3-D showed that adding rejuvenators did improve the flexibility of the N50 mix. However, its effect became less significant as the dosage was increased. The opposite effect was experienced for potential rutting resistance; highlighting the importance of incorporating an I-BMD analysis to mix performance criteria.
- 6% rejuvenator by weight of the binder content, appears to be the optimal dosage regarding acceptable FI and rut depth, and without experiencing excessive behavior changes between UA and STA conditions.
- Although the analysis of SIP values has been adopted by different agencies, this study showed that the method is prone to significant differences due to the inconsistencies of defining the limits of the creep and stripping phases. An analysis based on model fitting appears to return more consistent results and should be further explored.

5.4 Recommendations for Future Research

From the results of this study, the following topics have been identified as research areas that could help on the advancement of performance-based testing and analysis for AC:

- I-BMD proves to be a powerful tool to discriminate between the performance of different AC mix types. However, refining the boundaries for the criteria of the tests is essential to raise the credibility of the method, and should be correlated to field performance.
- In this study, homogeneity of rejuvenator-mix is assumed, but this is an unrealistic scenario that could influence test outcomes and should be an area for future research.
- Additional recycling agents and modifiers for AC must be investigated.
- Further research into the application of model fitting methods to assess moisture resistance is recommended to improve the accuracy and consistency of the results.

REFERENCES

1. Berg, C. N., U. Deichmann, Y. Liu, and H. Selod. *Transport Policies and Development.* The Journal of Development Studies, Vol. 53, No. 4, 2017, pp. 465–480.

2. American Society of Civil Engineers. *2017 Infrastructure Report Card.* https://www.infrastructurereportcard.org/, Accessed Jan. 1, 2018.

3. CEBR. *The Future Economic and Environmental Costs of Gridlock in 2030*. London, UK, 2014.

4. Texas Department of Transportation. *TxDOT Glossary*. Austin, TX, 2013.

5. Park, H. J., and Y. R. Kim. *Primary Causes of Cracking of Asphalt Pavement in North Carolina: Field Study*. International Journal of Pavement Engineering, Vol. 16, No. 8, 2014, pp. 684–698.

6. Anderson, R. M., G. N. King, D. I. Hanson, and P. B. Blankenship. *Evaluation of the Relationship between Asphalt Binder Properties and Non-Load Related Cracking*. Journal of the Association of Asphalt Pavement Technologists, Vol. 80, 2011, pp. 662–663.

7. Wu, Z., L. Mohammad, L. Wang, and M. Mull. *Fracture Resistance Characterization of Superpave Mixtures Using the Semi-Circular Bending Test*. Journal of ASTM International, Vol. 2, No. 3, 2005, pp. 1–15.

8. Pszczoła, M., M. Jaczewski, C. Szydłowski, J. Judycki, and B. Dołżycki. *Evaluation of Low Temperature Properties of Rubberized Asphalt Mixtures*. Procedia Engineering, Vol. 172, 2017, pp. 897–904.

9. Wu, S., K. Zhang, H. Wen, J. Devol, and K. Kelsey. *Performance Evaluation of Hot Mix Asphalt Containing Recycled Asphalt Shingles in Washington State*. Journal of Materials in Civil Engineering, Vol. 4, No. 1, 2016, pp. 1–10.

10. Motter, J. S., L. F. Rosemback Miranda, L. L. Bariani Bernucci. *Performance of Hot Mix Asphalt Concrete Produced with Coarse Recycled Concrete Aggregate*. Journal of Materials in Civil Engineering, Vol. 27, No. 11, 2015, pp. 1–7.

11. Vallerga, B. A., and W. R. Lovering. *Evolution of the Hveem Stabilometer Method of Designing Asphalt Paving Mixtures*. Journal of the Association of Asphalt Pavement Technologists, Vol. 54, 1985, pp. 243–265.

12. ASTM D5148-10. *Standard Test Method for Centrifuge Kerosine Equivalent*. ASTM International, West Conshohocken, PA, 2010.

13. ASTM D1560-15. *Standard Test Methods for Resistance to Deformation and Cohesion of Bituminous Mixtures by Means of Hveem Apparatus.* ASTM International, West Conshohocken, PA, 2015

14. FHWA. *Superpave Mixture Design Guide - WesTrack Forensic Team Consensus Report*. Federal Highway Administration, Washington, DC, 2001.

15. National Highway Institute. *Superpave Fundamentals*. Washington, DC, 2000.

16. Asphalt Institute. *Manual Series No. 2 (MS-2) Mix Design Methods for Asphalt Concrete and Other Hot Mix Types*. Lexington, KY, 1993.

17. Aljassar, A. H., M. A. Ali, and A. Alzaabi. *Modeling Marshall Test Results for Optimum Asphalt-Concrete Mix Design*. Kuwait Journal of Science and Engineering, Vol. 29, No. 1, 2002, pp. 181–195.

18. ASTM D6927-15. *Standard Test Method for Marshall Stability and Flow of Asphalt Mixtures*. ASTM International, West Conshohocken, PA, 2015.

19. Brown, S. F., K. E. Cooper, and G. R. Pooly. *Mechanical Properties of Bituminous Materials for Pavement Design*. Proceedings of the Second Eurobitume Symposium, Cannes, 1981.

20. Roberts, F. L., L. N. Mohammad, and L. B. Wang. *History of Hot Mix Asphalt Mixture Design in the United States*. Journal of Materials in Civil Engineering, Vol. 14, No. 4, 2002, pp. 279–293.

21. Brown, E. R., and S. A. Cross. *A National Study of Rutting in Hot Mix Asphalt (HMA) Pavements*. NCAT Report 92-05, Auburn, AL, 1992.

22. FHWA Highway Quality Compendium. *Asphalt's Generation of Change.* https://www.fhwa.dot.gov/construction/pubs/hif07012/23.cfm. Accessed Apr. 4, 2018.

23. Asphalt Institute Institute. *Superpave Series No. 2 (SP-2) Superpave Mix Design. Asphalt Institute*. Lexington, KY, 2001.

24. Mohammadafzali, M., H. Ali, J. A. Musselman, G. A. Sholar, S. Kim, and T. Nash. *Long-Term Aging of Recycled Asphalt Binders: A Laboratory Evaluation Based on Performance Grade Tests*. Proceedings of the International Airfield and Highway Pavements Conference 2015, Miami, FL, 2015.

25. Asphalt Institute. *Manual Series No. 22 (MS-22) Construction of Hot Mix Asphalt Pavements*. Asphalt Institute, 2001.

26. Cominsky, R., R. B. Leahy, and E. T. Harrigan. *Level One Mix Design: Materials Selection, Compaction, and Conditioning*. SHRP Report A-407, Washington, DC, 1994.

27. AASHTO M323. *Standard Specification for Superpave Volumetric Mix Design*. American Association of State Highway and Transportation Officials, Washington, DC, 2013.

28. AASHTO R35. *Practice for Superpave Volumetric Design for Hot Mix Asphalt (HMA)*. American Association of State Highway and Transportation Officials, Washington, DC, 2017.

29. Christensen, D. W., and R. F. Bonaquist. *Volumetric Requirements for Superpave Mix Design*. NCHRP Report 567, Washington, DC, 2006.

30. AASHTO 283-14. *Standard Method of Test for Resistance of Compacted Asphalt Mixtures to Moisture-Induced Damage*. American Association of State Highway and Transportation Officials, Washington, DC, 2014.

31. Cominsky, R., G. Huber, T. Kennedy, and M. Anderson. *The Superpave Mix Design Manual for New Construction and Overlays*. SHRP Report A-407, Washington, DC, 1994.

32. Zhou, F., S. Hu, and T. Scullion. *Integrated Asphalt (Overlay) Mixture Design, Balancing Rutting and Cracking Requirements*. Texas Transportation Institute, Report No. FHWA/TX-06/0-512-1, College Station, TX, 2006.

33. Brown, D. *Superpave Enters the Modification Era*. Better Roads, Vol. 75, No. 9, 2005, pp. 30–37.

34. Buchanan, S. *Balanced Mix Design Task Force: Update of Activities*. NAPA Asphalt Mix ETG Meeting, Salt Lake City, UT, 2017.

35. NCHRP 20-07/Task 406. *Development of a Framework for Balanced Asphalt Mixture Design*. http://apps.trb.org/cmsfeed/TRBNetProjectDisplay.asp?ProjectID=4324. Accessed Jan. 1, 2018.

36. Wisconsin DOT, *Flexible Pavement Research Project 0092-16-06*. http://wisconsindot.gov/Pages/about-wisdot/research/flex-pave.aspx. Accessed Jan. 1, 2018.

37. Texas DOT. *Develop Guidelines and Design Program for Hot-Mix Asphalts Containing RAP, RAS, and Other Additives through a Balanced Mix-Design Process*. https://library.ctr.utexas.edu/Presto/content/Detail.aspx?ctID=UmVzZWFyY2gtaW4tUHJvZ3

Jlc3NfMTExMjY=&rID=NTQ0&ssid=c2NyZWVuSURfMTgxMTY=. Accessed Jan. 1, 2018.

38. Zhou, F., D. Newcomb, C. Gurganus, S. Banihashemrad, E. S. Park, M. Sakhaeifar, and R. L. Lytton. *Experimental Design for Field Validation of Laboratory Tests to Assess Cracking Resistance of Asphalt Mixtures*. NCHRP Report 9-57, College Station, Texas, 2016.

39. Underwood, B. S. *Use of Models to Enhance the Durability of Asphalt Pavements*. Transportation Research Circular: Enhancing the Durability of Asphalt Pavements, 2013, pp. 18–32.

40. Dong, Q., X. Jiang, B. Huang, and S. H. Richards. *Analyzing Influence Factors of Transverse Cracking on LTPP Resurfaced Asphalt Pavements through NB and ZINB Models*. Journal of Transportation Engineering, Vol. 139, No. 9, 2013, pp. 889–895.

41. Hass, R., F. Meyer, G. Assaf, and H. Lee. *A Comprehensive Study of Cold Climate Airport Pavement Cracking*. Journal of the Association of Asphalt Pavement Technologists, Vol. 56, 1987, pp. 198–245.

42. Monismith, C. L., and N. F. Coetzee. *Reflection Cracking: Analysis, Laboratory Studies and Design Consideration*. Journal of the Association of Asphalt Pavement Technologists, Vol. 49, 1980, pp. 268–313.

43. ARA. *Guide for Mechanistic Empirical Design of New and Rehabilitated Pavement Structures*. NCHRP Report 1-37A, Washington, DC, 2004.

44. Roque, R., J. Zou, Y. R. Kim, C. Baek, S. Thirunavukkarasu, B. S. Underwood, and M. N. Guddati. *Top-Down Cracking of Hot-Mix Asphalt Layers: Models for Initiation and Propagation*. NCHRP Report 1-42, Washington, DC, 2010.

45. Drakos, C. A., R. Roque, B. Birgisson, and M. Novak. *Identification of a Physical Model to Evaluate Rutting Performance of Asphalt Mixtures*. Journal of ASTM International, Vol. 2, No. 3, 2005, pp. 156–176.

46. White, T., J. E. Haddock, A. Hand, and H. Fang. *Contributions of Pavement Structural Layers to Rutting of Hot Mix Asphalt Pavements*. NCHRP Report 468, Washington, DC, 2002.

47. Chen, J., and S. Wei. *Engineering Properties and Performance of Asphalt Mixtures Incorporating Steel Slag*. Construction and Building Materials, Vol. 128, 2016, pp. 148–153.

48. Chen, J. S., W. Hsieh, and M. C. Liao. *Effect of Coarse Aggregate Shape on Engineering Properties of Stone Mastic Asphalt Applied to Airport Pavements*. International Journal of Pavement Research and Technology, Vol. 6, No. 5, 2013, pp. 595–601.

49. Mokhtari, A., and F. Moghadas Nejad. *Mechanistic Approach for Fiber and Polymer Modified SMA Mixtures*. Construction and Building Materials, Vol. 36, 2012, pp. 381–390.

50. Zaumanis, M., R. B. Mallick, and R. Frank. *100% Recycled Hot Mix Asphalt: A Review and Analysis*. Resources, Conservation and Recycling, Vol. 92, 2014, pp. 230–245.

51. Al-Qadi, I. L., M. Elseifi, and S. H. Carpenter. *Reclaimed Asphalt Pavement - A Literature Review*. Illinois Center for Transportation, Report No. FHWA-ICT-07-001, Rantoul, IL, 2007.

52. Al-Qadi, I. L., I. M. Abuawad, H. Dhasmana, A. R. Coenen, and J. S. Trepanier. *Effects of Various Asphalt Binder Additives/Modifiers on Moisture-Susceptible Asphaltic Mixtures*. Illinois Center for Transportation, Report No. FHWA-ICT-14-004, Rantoul, IL, 2014.

53. Sebaaly, P. E., E. Hitti, and D. Weitzel. *Effectiveness of Lime in Hot-Mix Asphalt Pavements*. Transportation Research Record: Journal of the Transportation Research Board, Vol. 1832, 2003, pp. 33–41.

54. Park, D. W., W. J. Seo, J. Kim, and H. V. Vo. *Evaluation of Moisture Susceptibility of Asphalt Mixture Using Liquid Anti-Stripping Agents*. Construction and Building Materials, Vol. 144, 2017, pp. 399–405.

55. Petersen, J., and P. Harnsberger. *Asphalt Aging: Dual Oxidation Mechanism and Its Interrelationships with Asphalt Composition and Oxidative Age Hardening*. Transportation Research Record: Journal of the Transportation Research Board, Vol. 1638, No. 1, 1998, pp. 47–55.

56. Kumbargeri, Y. S., and K. P. Biligiri. *A Novel Approach to Understanding Asphalt Binder Aging Behavior Using Asphaltene Proportion as a Performance Indicator*. Journal of Testing and Evaluation, Vol. 44, No. 1, 2016, pp. 439–449.

57. Petersen, J., J. F. Branthaver, R. E. Robertson, P. M. Harnsberger, J. J. Duvall, and E. K. Ensley. *Effect of Physicochemical Factors on Asphalt Oxidation Kinetics*. Transportation Research Record: Journal of the Transportation Research Board, Vol. 1391, 1993, pp. 1–10.

58. Liu, M. M., M. S. Lin, J. M. Chaffin, R. R. Davison, C. J. Glover, and J. A. Bullin. *Oxidation Kinetics of Asphalt Corbett Fractions and Compositional Dependence of Asphalt Oxidation*. Transportation Research Record: Journal of the Transportation Research Board, Vol. 1638, 1998, pp. 40–46.

59. Petersen, J. C., and R. Glaser. *Asphalt Oxidation Mechanisms and the Role of Oxidation Products on Age Hardening Revisited*. Road Materials and Pavement Design, Vol. 12, No. 4, 2011, pp. 795–819.

60. Yu, X., M. Zaumanis, S. Dos Santos, and L. D. Poulikakos. *Rheological, Microscopic, and Chemical Characterization of the Rejuvenating Effect on Asphalt Binders*. Fuel, Vol. 135, 2014, pp. 162–171.

61. Al-Qadi, I. L., H. Ozer, J. Lambros, A. El-Khatib, P. Singhvi, T. Khan, J. Rivera-Perez, and B. Doll. *Testing Protocols to Ensure Performance of High Asphalt Binder Replacement Mixes Using RAP and RAS*. Illinois Center for Transportation, Report No. FHWA-ICT-15-017, Rantoul, IL, 2015.

62. Ozer, H., I. L. Al-Qadi, P. Singhvi, T. Khan, J. Rivera-Perez, and A. El-Khatib. *Fracture Characterization of Asphalt Mixtures with High Recycled Content Using Illinois Semicircular Bending Test Method and Flexibility Index*. Transportation Research Record: Journal of the Transportation Research Board, Vol. 2575, 2016, pp. 130–137.

63. Ozer, H., I. L. Al-Qadi, J. Lambros, A. El-Khatib, P. Singhvi, and B. Doll. *Development of the Fracture-Based Flexibility Index for Asphalt Concrete Cracking Potential Using Modified Semi-Circle Bending Test Parameters*. Construction and Building Materials, Vol. 115, 2016, pp. 390–401.

64. Tran, N., A. Taylor, and R. Willis. *Effect of Rejuvenator on Performance Properties of HMA Mixtures with High RAP and RAS Contents*. NCAT Report 12-05, Auburn, AL, 2012.

65. Karlsson, R., and U. Isacsson. *Investigations on Bitumen Rejuvenator Diffusion and Structural Stability*. Journal of the Association of Asphalt Pavement Technologists, Vol. 72, 2003, pp. 463–501.

66. Zaumanis, M., R. B. Mallick, R. Frank, L. Poulikakos, and R. Frank. *Influence of Six Rejuvenators on The Performance Properties of Reclaimed Asphalt Pavement (RAP) Binder and 100% Recycled Asphalt Mixtures*. Construction and Building Materials, Vol. 69, 2014, pp. 538–550.

67. Nahar, S., J. Qiu, A. Schmets, E. Schlangen, M. Shirazi, M. van de Ven, G. Schitter, and A. Scarpas. *Turning Back Time: Rheological and Microstructural Assesment of Rejuvenated Bitumen*. Transportation Research Record: Journal of the Transportation Research Board, Vol. 2444, 2014, pp. 52–62.

68. Ali, A. W., Y. A. Mehta, A. Nolan, C. Purdy, and T. Bennert. *Investigation of The Impacts of Aging and RAP Percentages on Effectiveness of Asphalt Binder Rejuvenators*. Construction and Building Materials, Vol. 110, 2016, pp. 211–217.

69. Shen, J., S. Amirkhanian, and B. Tang. *Effects of Rejuvenator on Performance-Based Properties of Rejuvenated Asphalt Binder and Mixtures*. Construction and Building Materials, Vol. 21, No. 5, 2007, pp. 958–964.

70. Ongel, A., and M. Hugener. *Impact of Rejuvenators on Aging Properties of Bitumen*. Construction and Building Materials, Vol. 94, 2015, pp. 467–474.

71. Lin, J., J. Hong, C. Huang, J. Liu, and S. Wu. *Effectiveness of Rejuvenator Seal Materials on Performance of Asphalt Pavement*. Construction and Building Materials, Vol. 55, 2014, pp. 63–68.

72. Carruth, W. D., and M. Mejí. *Hot In-Place Asphalt Recycling for Small Repairs on Airfields in Remote Setting*s. International Journal of Pavement Research and Technology, Vol. 8, No. 6, 1997, pp. 395–402.

73. Im, S., F. Zhou, R. Lee, and T. Scullion. *Impacts of Rejuvenators on Performance and Engineering Properties of Asphalt Mixtures Containing Recycled Material*s. Construction and Building Materials, Vol. 53, 2014, pp. 596–603.

74. NCAT. *Researchers Explore Multiple Uses of Rejuvenators*. Asphalt Technology News, Vol. 26, No.1, 2014, pp.7–8.

75. NAPA. *Designing and Constructing SMA Mixtures – State-of-the-Practice*. Lanham, MD, 2002.

76. Root, R. *Investigation of the use of Open-Graded Friction Courses in Wisconsin*. Wisconsin Highway Research Program, Report No. 09-01, Madison, WI, 2009.

77. Michael, L., G. Burke, and C. W. Schwartz. *Performance of Stone Matrix Asphalt Pavements in Maryland*. Journal of the Association of Asphalt Pavement Technologists, Vol. 72, 2003, pp. 287–314.

78. Brown, E. R., J. E. Haddock, and E. R. Brown. *Performance of Stone Matrix Asphalt (SMA) Mixtures in the United States*. NCAT Report 97-1 Auburn, AL, 1997.

79. Wu, S., H. Wen, S. Chaney, K. Littleton, and S. Muench. *Evaluation of Long-Term Performance of Stone Matrix Asphalt in Washington State*. Journal of Performance of Constructed Facilities, Vol. 31, No. 1, 2017, pp. 1–8.

80. Hao, D., and M. Won. *CAM and SMA Mixtures to Delay Reflective Cracking on PCC Pavements*. Construction and Building Materials, Vol. 96, 2015, pp. 226–237.

81. Al-Qadi, I. L., S. Son, and S. H. Carpenter. *Development of an Economical, Thin, Quiet, Long-Lasting, High Friction Surface Layer, Volume 1: Mix Design and Lab Performance Testing*. Illinois Center for Transportation, Report No. FHWA-ICT-13-001, Rantoul, IL, 2013.

82. Al-Qadi, I. L., J. Baek, Z. Leng, H. Wang, M. Doyen, J. Kern, and S. L. Gillen. *Short-Term Performance of Modified Stone Matrix Asphalt (SMA) Produced with Warm Mix Additives*. Illinois Center for Transportation, Report No. ICT-12-001, Rantoul, IL, 2012.

83. Pettinari, M., B. Schmidt, B. B. Jensen, and O. Hededal. *New Surface Layers with Low Rolling Resistance Tested in Denmark*. Asphalt Pavements - Proceedings of the International Conference on Asphalt Pavements, ISAP 2014, Vol. 1, 2014, pp. 323–332.

84. Pettinari, M., B. B. Lund-Jensen, and B. Schmidt. *Low Rolling Resistance Pavements in Denmark*. 6th Eurasphalt & Eurobitume Congress, Prague, 2016.

85. ASTM D6373-16. *Standard Specification for Performance Graded Asphalt Binder*. ASTM International, West Conshohocken, PA, 2016.

86. ASTM D7405-15. *Standard Test Method for Multiple Stress Creep and Recovery (MSCR) of Asphalt Binder Using a Dynamic Shear Rheometer*. ASTM International, West Conshohocken, PA, 2015.

87. D'Angelo, J., R. Q. Kluttz, R. Dongre, and K. Stephens. *Revision of the Superpave High Temperature Binder Specification: The Multiple Stress Creep Recovery Test*. Journal of the Association of Asphalt Pavement Technologists, Vol. 76, 2007, pp. 123–162.

88. AASHTO R30. *Standard Practice for Mixture Conditioning of Hot Mix Asphalt (HMA)*. American Association of State Highway and Transportation Officials, Washington, DC, 2015.

89. AASHTO TP124. *Standard Method of Test for Determining the Fracture Potential of Asphalt Mixtures Using Semicircular Bend Geometry (SCB) at Intermediate Temperature*. American Association of State Highway and Transportation Officials, Washington, DC, 2016.

90. AASHTO T324-16. *Standard Method of Test for Hamburg Wheel - Track Testing of Compacted Hot Mix Asphalt (HMA).* American Association of State Highway and Transportation Officials, Washington, DC, 2016.

91. Singhvi, P., H. Ozer, and I. L. Al-Qadi. *Environmental and Functional Benefits and Trade-Offs of Hot In-Place Recycling Treatment Techniques*. Center for Highway Pavement Preservation, Report No. ICT-17-001, Okemos, MI, 2016.

92. Al-Qadi, I. L., D. L. Lippert, S. Wu, H. Ozer, G. Renshaw, T. R. Murphy, A. Butt, S. Gundapuneni, J. S. Trepanier, J. W. Vespa, I. M. Said, A. F. Espinoza-Luque, and F. R. Safi. *Utilizing Lab Tests to Predict Asphalt Concrete Overlay Performance*. Illinois Center for Transportation, Report No. FHWA-ICT-17-020, Rantoul, IL, 2017.

93. Wu, S., I. L. Al-Qadi, D. L. Lippert, H. Ozer, A. F. Espinoza-Luque, and F. R. Safi. *Early-Age Performance Characterization of Hot-Mix Asphalt Overlay with Varying Amounts of Asphalt Binder Replacement*. Construction and Building Materials, Vol. 153, 2017, pp. 294–306.

94. Maxwell, B. *An Analysis of Impact Factors on the Illinois Flexibility Index Test*. Urbana, Il: MS Thesis University of Illinois Urbana-Champaign, 2016.

95. Rivera-Perez, J. *Effect of Specimen Geometry and Test Configuration on the Fracture Process Zone for Asphalt Materials*. Urbana, Il: MS Thesis University of Illinois Urbana-Champaign, 2017.

96. Yin, F., E. Arambula, R. Lytton, A. Martin, and L. Cucalon. *Novel Method for Moisture Susceptibility and Rutting Evaluation Using Hamburg Wheel Tracking Test*. Transportation Research Record: Journal of the Transportation Research Board, Vol. 2446, 2014, pp. 1–7.

97. Chaturabong, P., and H. U. Bahia. *The Evaluation of Relative Effect of Moisture in Hamburg Wheel Tracking Test*. Construction and Building Materials, Vol. 153, 2017, pp. 337–345.

98. Mohammad, L. N., M. Elseifi, W. Cao, A. Raghavendra, and M. Ye. *Evaluation of Various Hamburg Wheel-Tracking Devices and AASHTO T 324 Specification for Rutting Testing of Asphalt Mixtures*. Road Materials and Pavement Design, Vol. 18, No. sup4, 2017, pp. 128–143.

99. Ozer, H., I. L. Al-qadi, E. Barber, E. Okte, Z. Zhu, and S. Wu. *Evaluation of I-Fit Results and Machine Variability Using MNRoad Test Track Mixtures*. Illinois Center for Transportation, Report No. FHWA-ICT-17-012, Rantoul, IL, 2017.

APPENDIX A: SMA AND N50 MIX DESIGNS

NCC Roads A/S
Laboratoriet
LAB 120 010303

ASFALTSPECIFIKATION

Asfalt spec.	**15993**	Udstedt dato	**13-06-2016**
Prod.sted	**Ejby Fabrik**	Erstatter spec.	
Kunde	**Selvfakturering VD**	Erstatter dato	
Entreprise	**Hldv. 619, Kalvehave, BEL21-2016, FVL**	Ordrenr	**3446013-160021**
Materiale	**SMA 8 ubelyst**	Receptnr.	**55310.02**

Bitumentype	**pen 70/100**		Bitumenindhold	**7,0**	%	Hulrums %	**2,7** %
Blødhedspunkt, K&R	**51**	°C	Stendensitet	**2,760**	g/cm³	Hulrums % i stenmat.	**19,1** %
Stabilitet		N	Marshall rumvægt	**2,400**	g/cm³	Bitumenfyldning	**86** %
V_b / V_s			Deformation		mm	Reflektionsfaktor	**0,080**

Sigteanalyse

Sigte mm	Gennemf. %
31,5	
22,4	
16	
11,2	**100**
8	**93**
5,6	**54**
4	**38**
2	**25**
1	**18**
,5	**14**
,25	**11**
,125	**9**
,063	**8,0**

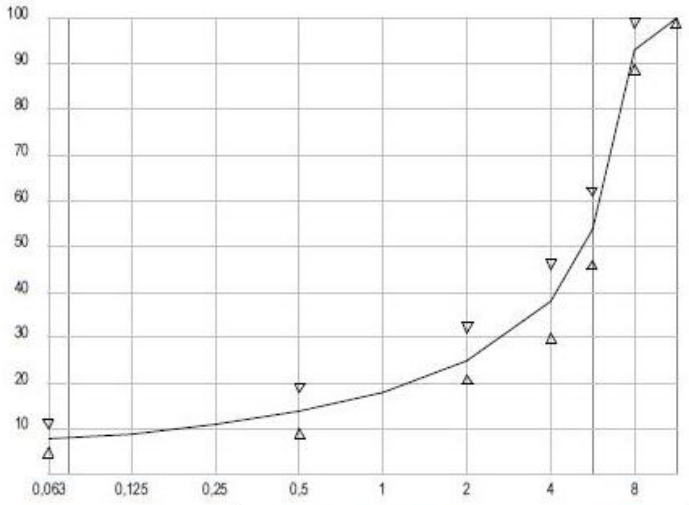

Komponenter

41,69% 5/8 klippegranit
11,63% 5/8 Labradorit
20,36% 2/5 klippegranit
11,63% Stenmel
11,63% Stenmel
1,50% Klæbeaktiv filler
1,20% Filler
0,35% Viatorp Fibre

Klæbning, mængde ca **300** g/m²
Klæbning, type **Sur emulsion**

Bemærkninger

Marshall 2x50 slag v/135 °C

Blanding 2 og 7

Korrektionsfaktor = 0,42

Laboratoriet, den 13. jun. 2016
Med venlig hilsen
Anne Grethe Pedersen

Figure A.1 Mix Design for SMA8 Ref

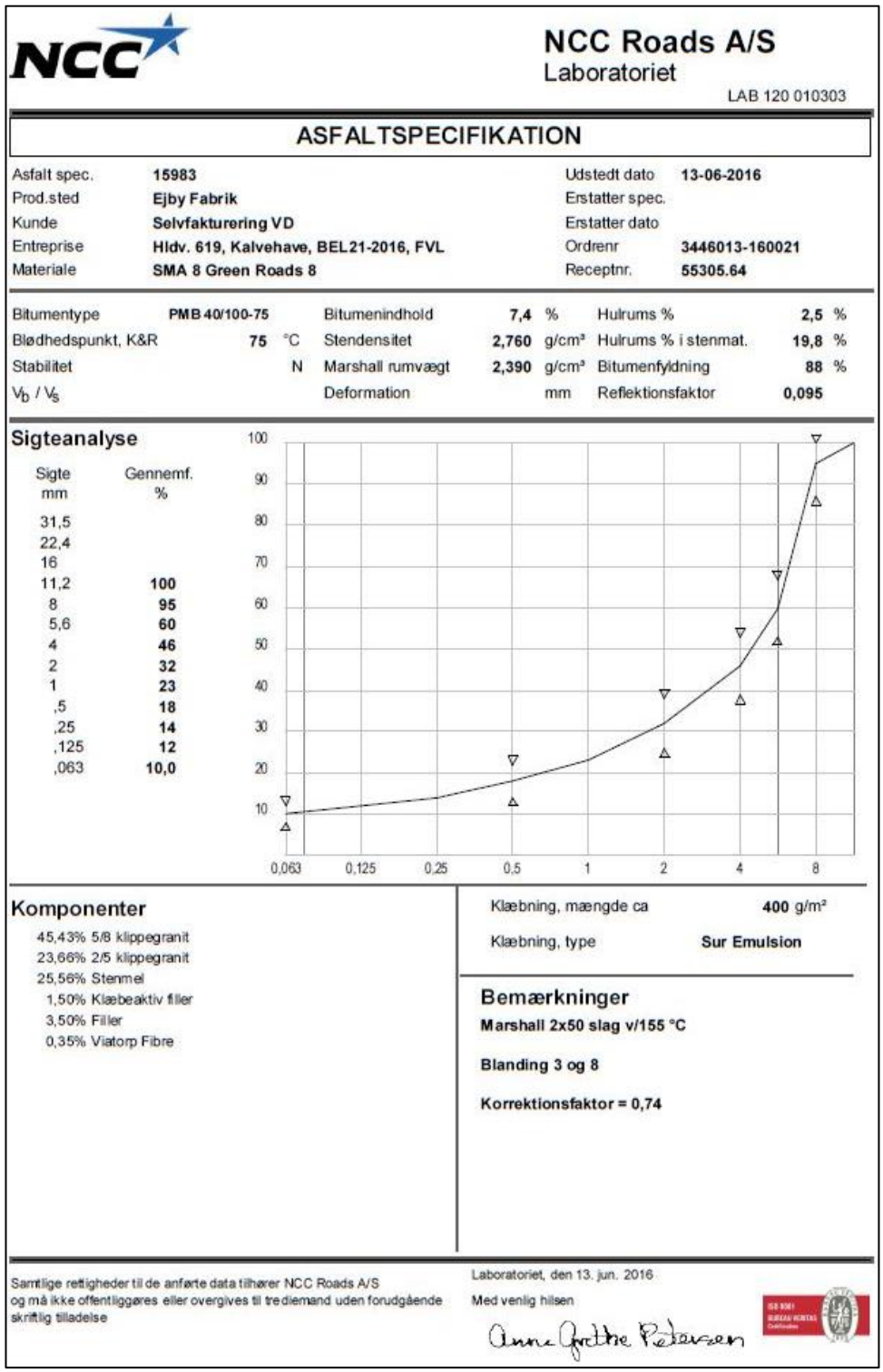

NCC Roads A/S
Laboratoriet
LAB 120 010303

ASFALTSPECIFIKATION

Asfalt spec.	15983	Udstedt dato	13-06-2016
Prod.sted	Ejby Fabrik	Erstatter spec.	
Kunde	Selvfakturering VD	Erstatter dato	
Entreprise	Hldv. 619, Kalvehave, BEL21-2016, FVL	Ordrenr	3446013-160021
Materiale	SMA 8 Green Roads 8	Receptnr.	55305.64

Bitumentype	PMB 40/100-75		Bitumenindhold	7,4	%	Hulrums %	2,5 %
Blødhedspunkt, K&R	75	°C	Stendensitet	2,760	g/cm³	Hulrums % i stenmat.	19,8 %
Stabilitet		N	Marshall rumvægt	2,390	g/cm³	Bitumenfyldning	88 %
V_b / V_s			Deformation		mm	Reflektionsfaktor	0,095

Sigteanalyse

Sigte mm	Gennemf. %
31,5	
22,4	
16	
11,2	100
8	95
5,6	60
4	46
2	32
1	23
,5	18
,25	14
,125	12
,063	10,0

Komponenter

45,43% 5/8 klippegranit
23,66% 2/5 klippegranit
25,56% Stenmel
1,50% Klæbeaktiv filler
3,50% Filler
0,35% Viatorp Fibre

Klæbning, mængde ca 400 g/m²
Klæbning, type Sur Emulsion

Bemærkninger

Marshall 2x50 slag v/155 °C

Blanding 3 og 8

Korrektionsfaktor = 0,74

Laboratoriet, den 13. jun. 2016
Med venlig hilsen
Anne Grethe Pedersen

Figure A.2 Mix Design for SMA8 COOEE

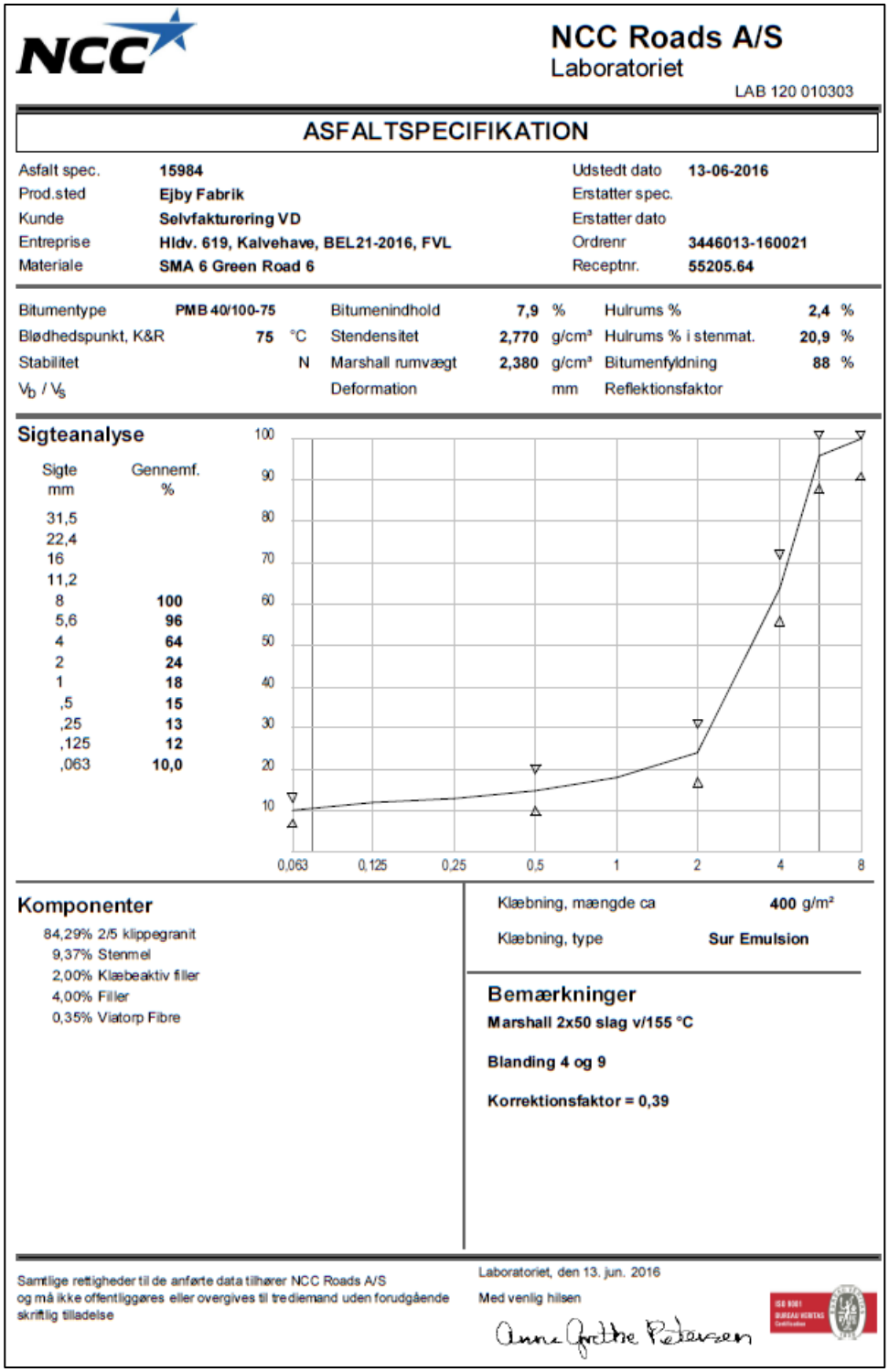

NCC Roads A/S
Laboratoriet
LAB 120 010303

ASFALTSPECIFIKATION

Asfalt spec.	**15984**	Udstedt dato	**13-06-2016**
Prod.sted	**Ejby Fabrik**	Erstatter spec.	
Kunde	**Selvfakturering VD**	Erstatter dato	
Entreprise	**Hldv. 619, Kalvehave, BEL21-2016, FVL**	Ordrenr	**3446013-160021**
Materiale	**SMA 6 Green Road 6**	Receptnr.	**55205.64**

Bitumentype	**PMB 40/100-75**		Bitumenindhold	**7,9**	%	Hulrums %	**2,4** %
Blødhedspunkt, K&R	**75**	°C	Stendensitet	**2,770**	g/cm³	Hulrums % i stenmat.	**20,9** %
Stabilitet		N	Marshall rumvægt	**2,380**	g/cm³	Bitumenfyldning	**88** %
V_b / V_s			Deformation		mm	Reflektionsfaktor	

Sigteanalyse

Sigte mm	Gennemf. %
31,5	
22,4	
16	
11,2	
8	**100**
5,6	**96**
4	**64**
2	**24**
1	**18**
,5	**15**
,25	**13**
,125	**12**
,063	**10,0**

Komponenter

84,29% 2/5 klippegranit
9,37% Stenmel
2,00% Klæbeaktiv filler
4,00% Filler
0,35% Viatorp Fibre

Klæbning, mængde ca **400** g/m²
Klæbning, type **Sur Emulsion**

Bemærkninger

Marshall 2x50 slag v/155 °C

Blanding 4 og 9

Korrektionsfaktor = 0,39

Laboratoriet, den 13. jun. 2016
Med venlig hilsen
Anne Grethe Pedersen

Figure A.3 Mix Design for SMA6 COOEE

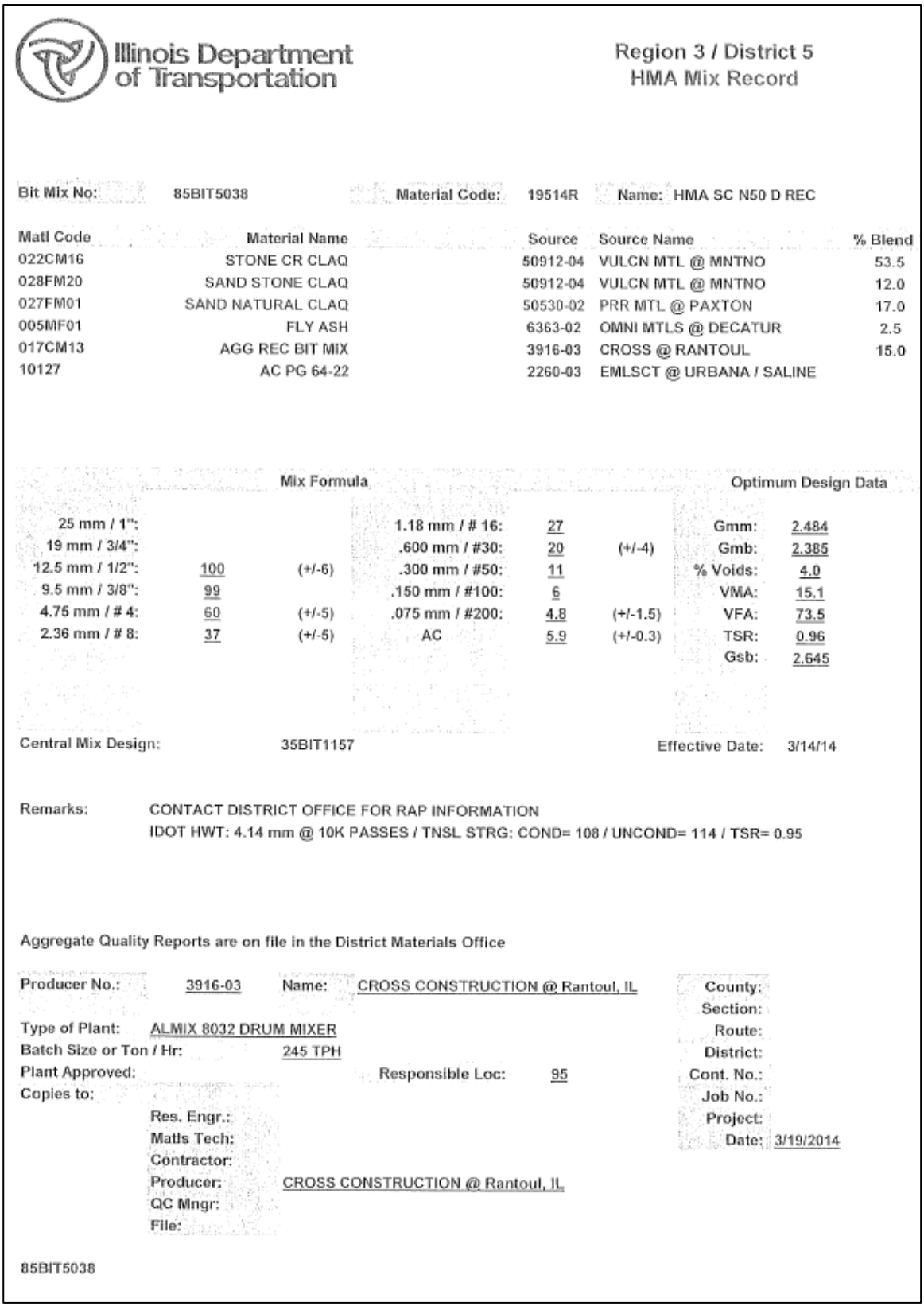

Illinois Department of Transportation

Region 3 / District 5
HMA Mix Record

Bit Mix No: 85BIT5038 Material Code: 19514R Name: HMA SC N50 D REC

Matl Code	Material Name	Source	Source Name	% Blend
022CM16	STONE CR CLAQ	50912-04	VULCN MTL @ MNTNO	53.5
028FM20	SAND STONE CLAQ	50912-04	VULCN MTL @ MNTNO	12.0
027FM01	SAND NATURAL CLAQ	50530-02	PRR MTL @ PAXTON	17.0
005MF01	FLY ASH	6363-02	OMNI MTLS @ DECATUR	2.5
017CM13	AGG REC BIT MIX	3916-03	CROSS @ RANTOUL	15.0
10127	AC PG 64-22	2260-03	EMLSCT @ URBANA / SALINE	

Mix Formula

						Optimum Design Data	
25 mm / 1":			1.18 mm / # 16:	27		Gmm:	2.484
19 mm / 3/4":			.600 mm / #30:	20	(+/-4)	Gmb:	2.385
12.5 mm / 1/2":	100	(+/-6)	.300 mm / #50:	11		% Voids:	4.0
9.5 mm / 3/8":	99		.150 mm / #100:	6		VMA:	15.1
4.75 mm / # 4:	60	(+/-5)	.075 mm / #200:	4.8	(+/-1.5)	VFA:	73.5
2.36 mm / # 8:	37	(+/-5)	AC	5.9	(+/-0.3)	TSR:	0.96
						Gsb:	2.645

Central Mix Design: 35BIT1157 Effective Date: 3/14/14

Remarks: CONTACT DISTRICT OFFICE FOR RAP INFORMATION
IDOT HWT: 4.14 mm @ 10K PASSES / TNSL STRG: COND= 108 / UNCOND= 114 / TSR= 0.95

Aggregate Quality Reports are on file in the District Materials Office

Producer No.: 3916-03 Name: CROSS CONSTRUCTION @ Rantoul, IL

Type of Plant: ALMIX 8032 DRUM MIXER
Batch Size or Ton / Hr: 245 TPH
Plant Approved: Responsible Loc: 95
Copies to:
Res. Engr.:
Matls Tech:
Contractor:
Producer: CROSS CONSTRUCTION @ Rantoul, IL
QC Mngr:
File:

County:
Section:
Route:
District:
Cont. No.:
Job No.:
Project:
Date: 3/19/2014

85BIT5038

Figure A.4 Mix Design for N50